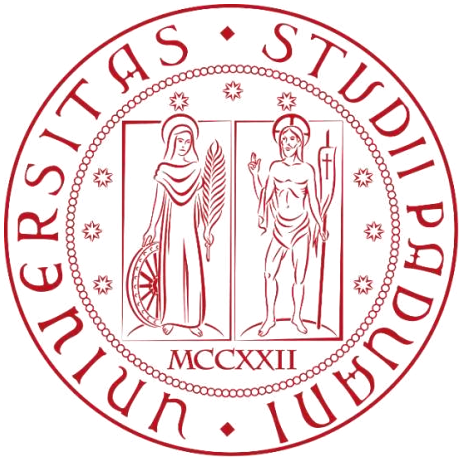

UNIVERSITA' DEGLI STUDI DI PADOVA

DIPARTIMENTO DI SCIENZE DEL FARMACO

CORSO DI LAUREA MAGISTRALE IN CHIMICA E TECNOLOGIA FARMACEUTICHE

TESI DI LAUREA

ESTABLISHMENT OF CULTURE CONDITIONS FOR PATIENT-DERIVED TUMOR EXPLANTS OF BASAL CELL CARCINOMA

RELATORE: PROF.SSA PATRIZIA POLVERINO DE LAURETO

Dipartimento di Scienze del Farmaco, Università degli Studi di Padova

CO-RELATORE: PROF. FRANÇOIS KUONEN

Service de Dermatologie, CHUV, Université de Lausanne

LAUREANDO: SOMMACAL FRANCESCO
Matricola: 1225908

Anno Accademico 2023/2024

Summary

1 Abstract

Basal Cell Carcinoma (BCC) is a very common type of cancer today; it derives from the Hedgehog pathway, a signaling way normally active during the embryonal phase that can be reactivated for the insurgence of a tumor. Despite being spread all around the world, no human cell lines exist to study BCC *in vitro* and primary tumor cells do not grow as the cells cannot culture and survive alone. Indeed, BCC cells need a specific architecture guaranteed by the stromal cells and the extracellular matrix. To overcome this problem, this study focuses on identifying the optimal culture medium for the culture of BCC-explants. The aim of this work is to find an environment that is the nearest possible to the physiological one and that it does not somehow affect the tumor characteristics to be able, in the future, to perform functional experiments *in vitro*, like drug screening. The two tested culture media were M154CF and Co-Culture Medium + Epidermal Growth Factor (CCM+EGF). The tumor explants were taken from three different patients and incubated for 24 hours in each condition. Next, different tests (morphology, proliferation, apoptosis and hedgehog pathway activation) were performed in parallel to compare the two culture conditions. Thanks to these, it was possible to have an overall picture of this pathology and how it could have been influenced by its environment. Through all the tests, several considerations are made based on the different marker scores that were obtained, conditioned by both the media and the tumor variant studied. Eventually, it was not possible to determine which culture medium was better. Still, this work opens the way to future studies that could help to find the best culture medium for Basal Cell Carcinoma.

2 Riassunto

Il Carcinoma Baso-cellulare (o Basalioma) è una tipologia di tumore alla pelle molto comune oggigiorno; prende origine dall'Hedgehog pathway, una via di segnalazione tipicamente attiva durante le prime fasi embrionali che può però essere riattivata per l'insorgenza di un tumore. Nonostante sia molto diffuso, non esistono linee cellulari per studiare il Basalioma *in vitro* e le cellule tumorali primarie non crescono siccome queste non possono crescere e sopravvivere da sole. Infatti, le cellule di Basalioma hanno bisogno di una specifica architettura, che viene garantita dalle cellule stromali e dalla matrice extracellulare. Per risolvere questo problema, questo studio si focalizza sul trovare il terreno di coltura ottimale per espianti umani di Carcinoma Baso-cellulare: in particolare, lo scopo di questo lavoro è quello di trovare l'ambiente il più vicino possibile a quello fisiologico e che, allo stesso tempo, non influenzi in qualche modo le caratteristiche intrinseche del tumore, in modo da eseguire in futuro degli esperimenti in vitro, come test con un farmaco. I due terreni di coltura testati sono stati M154CF e Co-Culture Medium + Epidermal Growth Factor (CCM+EGF). Gli espianti tumorali sono stati presi da tre pazienti differenti e incubati per 24 ore in ciascuna condizione. Successivamente, vari test (morfologia, proliferazione, apoptosi e riattivazione dell'Hedgehog pathway) sono stati fatti in parallelo per comparare le condizioni nei due terreni. Grazie a questi è stato possibile avere un quadro generale di questa patologia e di come possa essere influenzata dopo l'incubazione nei due terreni di coltura. Dopo questi test, alcune considerazioni sono state fatte, basate sui diversi risultati di ciascun marcatore ottenuti, i quali sono stati condizionati sia dai terreni stessi che dalla tipologia di tumore studiata. Infine, non è stato possibile determinare quale terreno di coltura fosse migliore. Nonostante ciò, questo lavoro apre la strada verso studi futuri che potrebbero trovare finalmente il terreno di coltura migliore per il Carcinoma Baso-cellulare.

3 Introduction

3.1 Skin

The Integumentary system is constituted mainly by the skin and the skin appendages. The skin (or cutis) is the heaviest organ in the human body, reaching 1.5-2 m^2 of surface[1]; also, it has different levels of thickness, going from 0.5 mm in the eyelids to 4 mm in the soles of the feet[2]. Thickness allows to discriminate through each skin area, alongside the folds and the presence of hair follicles and glands.

The cutis is a crucial component of our organism because it represents the first shield for chemical, biological and physical agents like chemicals, fungi and radiations, and it protects the body from mechanical stresses and traumas[3]. Moreover, it maintains the body temperature constant, and it prevents dehydration, thanks to the sweat glands. They are divided into apocrine and eccrine types: the eccrine ones, especially, are in higher number compared to the apocrine glands, and must continuously bathe the skin surface, producing a mixture of water and salt. Also, for thermoregulation, they release latent heat from the evaporation of water with the apocrine glands, and let the skin become more acidic to prevent the colonization and growth of microorganisms[3]. The skin has a pH around 5.4-5.9, this makes it a hostile environment for pathogens. Consequently, the great difference in pH with the blood (pH 7.4) is a good second defensive line in case microbes manage to enter the circulation.

The cutis is composed by three main components: from the outside to the inside, we have the epidermis, a multilayered epithelium composed by cells bound together by tight junctions[4]; these form the first mechanical barrier of the body and impede the passage of many substances. Under the epidermis there is the derma, a connective tissue that gives all the nutrients and receives all the epidermis metabolites through the dermal papillae[5]; the epidermis and the derma are divided by the dermo-epidermal junction, which keeps the two layers attached and prevents the passage of molecules with molecular weight greater

than 40 kDa. The last layer is represented by the hypoderm, another connective tissue enriched in adipocytes [Fig. 1].

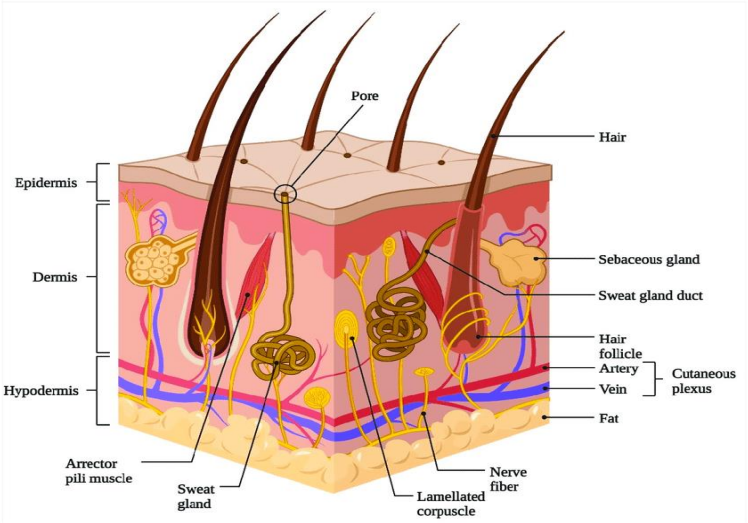

Fig. 1: Skin composition; the epidermis, the derma and the hypoderm constitute the cutis: the epidermis is the first level for defense against any kind of external insult, the derma contains the hair follicles and the glands, plus it hosts the blood and lymphatic vessels to keep the skin cells alive; the hypoderm is responsible for thermoregulation. This picture was taken from [6].

The skin appendages take also part to the integumentary system and comprehend mainly the hair follicles, the sebaceous glands and the sweat glands.

3.1.1 Epidermis

The epidermis is an internal lining of epithelial tissue composed by different types of cells. The most predominant ones are the keratinocytes[7]: these are cells which live nearly 14 days, starting from the deepest layers of the epidermis, where they proliferate continuously. After that, they start to emerge until the external surface, differentiating themselves and producing Keratin, a filamentous protein that gives the typical endurance of the skin and let it resist from almost any mechanical stress. Once they reach the superficial layer of the skin, the keratinocytes die and transform themselves in corneocytes[5], which have the highest amount of Keratin. It takes totally four weeks from the birth of a keratinocytes until its removal from the external layer of the epidermis[2].

The epidermis is constituted mainly by five different sublayers:

- Stratum basale: it is formed by only one layer of basal cells, important because they permit the continuous renewal of the keratinocytes, which proliferate mitotically and start to go up until ultimate transformation in corneocytes. In the stratum basale the melanocytes also take place, peculiar cells that are responsible for the color of the skin[5]. Thanks to specific organelles called melanosomes, they can produce two different molecules, the Eumelanin, and the Pheomelanin, which determine the ethnicity of each human being. Based on which molecule is produced and in which amount, the skin can have many different pigmentations, which can be subjected to hormones activity, light exposure and alimentation. In the keratinocytes, the pigment granules furnished by the melanocytes, after solar irradiation, form a barrier that prevents or diminishes the UV penetration, preventing any damage to the DNA[8].
- Stratum spinosum: it is composed by multiple layers of keratinocytes that aggregate and form bundles that can contain the melanocytes. The external keratinocytes of the stratum spinosum organize themselves in 0,2 μm granules that are expelled in the intercellular space, forming an impermeable barrier to water. The most external cells of this layer produce also Involucrin, which starts the cornification process[9].
- Stratum granulosum: it is the transition layer from living to dead keratinocytes. Here, the cells are flat and assemble one another very tightly, and the nuclei start to disappear. Plus, in the cytoplasm the cells start to form the Keratohyalin granules. They are formed by Filaggrin, which binds Keratin and stabilizes it with disulfide bonds, forming an impermeable shield[2].
- Stratum lucidum: it is a transparent layer of dead keratinocytes. Here, the cells, instead of Keratin, contain Eleidin, an intracellular protein which gives the transparent look of the stratum lucidum. Sometimes the stratum lucidum cannot be seen in the skin stratification[5].

- Stratum corneum: this is the last layer of the epidermis. The keratinocytes are already dead, and they are formed by 80 % of Keratin. They are stabilized by strong disulfide bonds and are covered by a layer of multilamellar organized lipids. In this state they measure 30-40 µm in diameter and 0.1-1.0 µm in thickness[8]. This represents the first barrier of the skin from mechanical traumas, biological and chemical insults; it also gives the ability to flex and move with the elements it is covering. The stratum corneum and granulosum collaborate to set the level of permeability for water. Fatty acids are also produced in the stratum corneum and are responsible for the acidification of the skin with the sweat glands.

The keratinocytes spend 14 days to pass through all the epidermis layers until cornification in the stratum corneum and other 14 days to desquamate and being removed. This entire process is called Cytomorphosis and can be influenced by other molecules like hormones and prostaglandins.

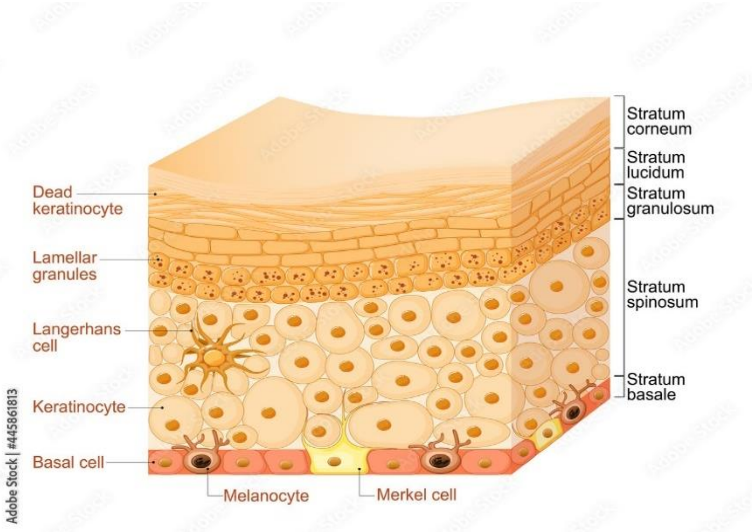

Fig. 2: Epidermis composition; the keratinocytes life cycle starts in the stratum basale where they proliferate, next they start to differentiate themselves, going up towards the surface. During their maturation, the amount of Keratin increases until they die in the stratum corneum, forming a strong barrier against pathogens and outer stress. This picture was taken from [10].

In addition to keratinocytes, there are other types of cells in the skin: Langerhans cells can be found in the stratum spinosum and represent the 3-4 % of all the epidermal cells. They are macrophages that originate from the bone marrow cells that move into the cutis and constitute the first line for skin immune defense[11]. In fact, they recognize, interiorize and exhibit the antigens to the lymphocytes, igniting eventually an immune response. Langerhans cells can migrate from the epidermis to the below derma but also in the lymphatic regions, defending the human body from biological antigens.

Finally, there are the Merkel cells: these are cells that take place most of all in the cutis with hair follicles presence between the epidermis and the derma, more specifically in the stratum basale, alongside the tactile nervous terminations. They have a roundish flat shape and within their cytoplasm they have many vesicles assembled near the cellular membrane. Here, they collaborate with non-myelinic nervous fiber and, together, they are responsible for the perception of tactile stimuli[12] [Fig. 2]. Glabrous skin is the most sensible part to tactile stimulation, and the sensibility grows considering distant limbs in the body, except for the face that has a high spatial acuity because of the presence of both myelinated and unmyelinated nerve fibers.

The epidermis is divided from the derma thanks to the dermo-epidermal junction, a tri-layered connective tissue that assures the oxygen delivery to the epidermal cells and the elimination of their catabolites. It is formed by the basal lamina, which is constituted by chained type Collagen fibers that guarantee tissue strength and elasticity, the lamina lucida, formed by adipocytes, whose role is to ensure that the epithelial cells are attached to the basal lamina, and the lamina fibroreticularis, responsible for the adhesion of epidermis and derma, thanks to the type VII Collagen fibers.

3.1.2 Derma

The derma is a dense white connective tissue made of intertwining bundles 1-2 mm thick[4], in which there can be found compounds like fibroblasts, macrophages and mast cells, fundamental during the inflammatory response.

Fibroblasts, especially, form an extracellular matrix made of Collagen, proteoglycans and elastic fibers which constitute the integrity of this tissue[7].

The derma also contains glycoproteins and peptidoglycans: peptidoglycans can be sulphurated, like heparan sulphate, dermatan sulphate and chondroitin sulphate, which make the derma layer compact and resistant, or non-sulphurated, like hyaluronic acid, responsible for the level of hydration in the connective tissue.

The derma is divided into two different layers:

- Papillary layer: it is strongly related to the above epidermis with which it interacts, and it is formed by conical protrusions, the dermal papillae. It also surrounds the hair follicles[4]. It is full of type III Collagen fibers interspersed with elastic fibers, which form extensions and facilitate the metabolic exchange with the epidermis. This layer has more cells than the next layer, but it is less dense.
- Reticular layer: it is marginally thicker than the papillary layer due to the numerous Collagen and elastic fibers that compose it. They have a larger diameter compared to the ones in the dermal layer and, depending on their orientation, they confer a great resistance towards the deformation of the skin, thanks to type I Collagen fibers [Fig. 3].

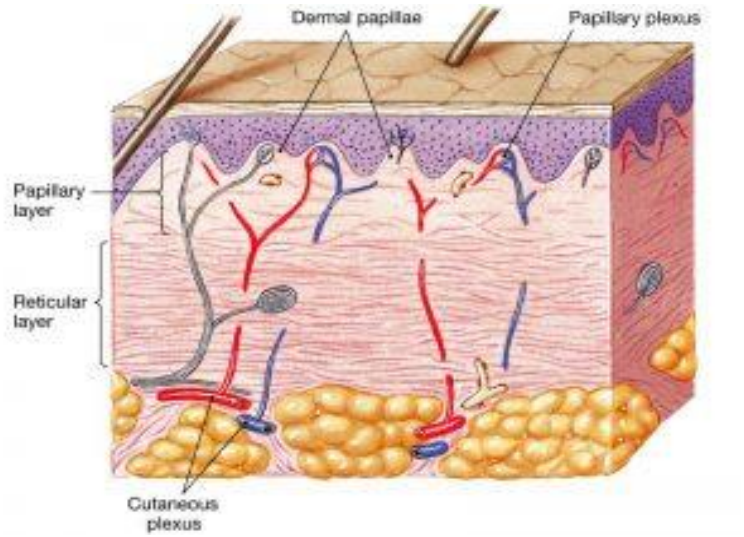

Fig. 3: Derma composition; the upper part is represented by the papillary layer, which is connected to the epidermis through the dermal papillae and exchange with it all the nutrients and metabolites. The lower part is the reticular layer, which is thicker and sustains the whole derma. This picture was taken from [13].

The dermis, like the epidermis, contains also hair follicles, sweat and sebaceous glands, lymphatic and blood vessels, but, deep down, it does not have a marked limit with which it separates from the lower hypoderm, on the contrary, the edges are not clear.

Based on what kind of vascular need the area of the tissue has, interconnecting anastomoses allow blood perfusion from close territories. At dermal layer, the skin introflections make room to both arterial and vein vessels, while the deeper lymphatic plexus is between the dermis and the hypoderm, forming a pattern that allows an efficient interstitial fluid turnover. Changes in any tissue property of the fibrous lamellar components can bring to surface buckling, resulting in wrinkles. Examples may be thinning of the dermis, thickening of the stratum corneum or, on the contrary, thinning of the epidermis, with loss of Collagen IV and VII at dermo-epidermal junction level[2]. In general, the loss of Elastin, main component of the elastic fibers, the degradation of Collagen and the changes in the interstitial fluid of the tissue lead to aging: Collagen is less soluble in aged skin but thickened and soluble if the cutis is sun-damaged, with Elastin that is deposited in the papillary dermis; this makes the

skin more fragile. Skin degeneration can be noticed also in the loss of its volume, that goes from 30 % at 50 years to 52 % at 80 years of age, studies say[4].

3.1.3 Hypoderm

The hypoderm (or subcutaneous) is the deepest layer of the skin, that puts it in contact with the most superficial layers of the bone and cartilage. Its thickness can vary from 0.5 cm, as in head and nose, to 2 cm, as in glutes and laps[8]. It is formed by loose connective tissue crammed with elastic fibers and adipocytes, which, if they are in large amounts, represent a great reserve of energy and form pockets that insulate and protect the skin. It acts as an endocrine organ, crucial for glucose homeostasis and lipid metabolism[5]. Moreover, it contains many immune cells, as proteoglycans and glycosaminoglycans. which attract the fluids in the tissue giving it mucous-like properties[7]. It is a thermal insulating layer, in fact fat is a poor conductor of heat, an interesting skill that the hypodermis exploits both to maintain heat inside the organism and, at the same time, to generate it through physical exercise, forming an intelligent balancing system to preserve the overall temperature of the body. The hypoderm also works as a cleavage between the skin and the lower components of the body, guaranteeing that they will slide on one another, while it acts a support for the whole integumentary system[4]. The deepest part of this layer is formed by fibers that coalesce and separate to form new vacuoles, creating a great 3D structure that maintains space and fibers conformation. The hypodermis also produces many mediators like growth factors, especially the Epidermal Growth Factor, which is crucial during the skin regeneration[7]. In fact, after a wound, it ignites a signal cascade that induce the regenerative process, and in general, it stimulates the keratinocytes proliferation, promoting the skin growth.

3.2 Skin appendages

3.2.1 Hair follicle

Hair follicles are flexible Keratin filaments distributed on the whole surface of the human body, except for the hairless skin components, which are the soles of the feet, the hand palms, the phalanx surfaces, the prepuce, the glans, the clitoris, the outer lips and the inner lips. The hair follicles' role is to protect the organism and, also, they are tactile receptors, thanks to the nervous terminal structure they dispose[14]. The number of hair follicles is fixed from day birth and there cannot be new ones during the lifetime of a human being. Each hair follicle is associated with a sebaceous gland, that takes place in an inner skin region called follicle collar and with which it forms the pilosebaceous complex[15]: the hair follicle, specifically, is created by a long narrow epidermal introflection in the skin, that becomes wide in the derma and it terminates with a structure called bulb.

Near the external surface there is the sebaceous gland, a structure that produces the sebum, a mixture of substances that acts as lubricant for the hair follicles and the epidermis, and, at the same time, protects the skin from humidity, drought and bacterial invasion[3] [Fig. 4].

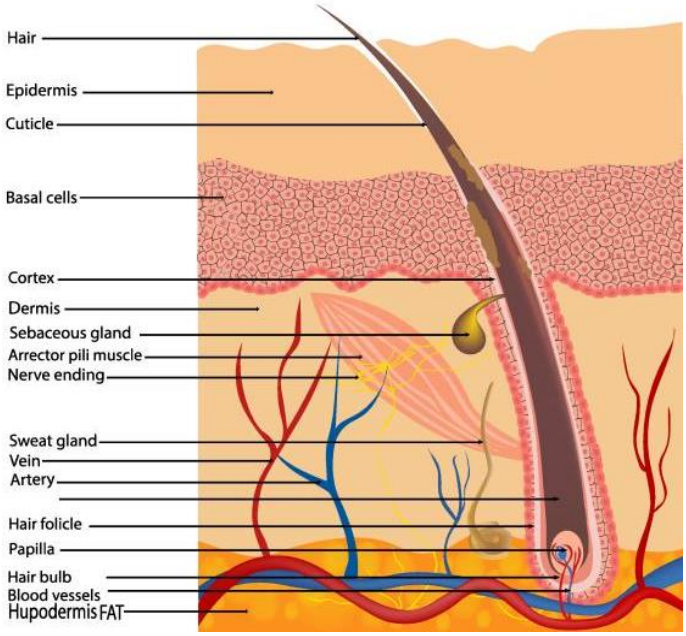

Fig. 4: Hair follicle structure; it starts with the formation of the space in which the hair will take place, then the real hair will grow until reaching the skin surface. To each hair follicle is associated one sebaceous gland that squeezes each time the hair is erected. This picture was taken from [16].

The introflection in the skin from which the hair follicle takes origin is an inside space in the follicular wall that is formed by an epithelium and an external layer of connective tissue (vitreous membrane), in straight contact with the surrounding derma. The vitreous membrane is made of two different layers, the first one, near the derma, is composed by longitudinal Collagen and elastic fibers, while the other one, close to the epidermis, is formed by circular Collagen fibers that, as the epidermis, give great strength to the entire structure. Among these fibers there are numerous non-myelinic nervous terminations responsible for the tactile sensibility of the hair follicle[8]. The connective tissue covers also the bulb, forming the hair papilla, a space that gives hospitality to the hair follicle.

The hair follicle can be divided into two areas: the superficial one, called shaft, and the deeper one that represents the root. The shaft is a 20-500 μm, keratin segment divided into three sublayers:

- Cuticula: it is a 2-4 μm thick and formed by quadrangular corneous scales that work like the keratinocytes; this sublayer protects the lower two ones, and it changes itself during the hair growth. It determines the hair opacity.
- Cortex: it is the pigmented part of the hair, and it is formed by elongated epidermal cornified elements that give strength to the whole hair, thanks also to the presence of specific fibrils.
- Medulla: it is formed by assembled polyhedric cells that are not largely cornified, thus being the most delicate part of the hair shaft[8].

The root is pretty much constituted as the shaft, with also an adding thin sheath outside the cuticula. In addition to this, it is constituted by two other sheets that cover the deepest part of the hair follicle: the first one is the external sheath of the root, which is in straight contact with the vitreous membrane, and it is considered as part of the epidermis. In fact, it is formed by a single layer of keratinocytes that further will become multilayered as they will approach the external surface; the second sheet is represented by the inner sheath of the root which can only be found in the deepest part of the follicle[17]. It is formed, in turn, by three sublayers: the first one is the Henle layer, formed by cells very adherent to the external sheath, the Huxley layer, composed by three lines of cornified cells, and third the internal sheath cuticula, formed by thin cornified scales. These three layers tend to desquamate at sebaceous gland level in favor of the root growth within the follicle collar.

The deepest part of the hair follicle is constituted by the bulb: it is placed at the end of the root, and it contributes to the formation and growth of the hair follicle. In particular, the growing portion of the bulb is localized around the dermal papilla, and it is composed by undifferentiated cells that form the bulb matrix. These will proliferate and migrate until they reach the cutaneous surface where they will distinguish themselves as elements of cuticula, cortex and medulla like the keratinocyte's differentiation. These cells will constitute the fundamental elements of the hair shaft, while the external cells will regroup and take part of the external and internal root sheaths[15]. In the upper part of the bulb

there can be found keratinocytes, responsible for the growth of the hair, but also melanocytes, which leave their pigment among the cortex fibers and within the medulla, giving the color of the hair follicle[15].

The hair follicle manages to be relaxed and erected thanks to the arrector pili muscle: it originates in the derma papillae, right below the epidermis, and it goes diagonally deep until it reaches the vitreous membrane of the hair follicles, under the sebaceous gland. The contraction of the arrector pili muscle provokes the compression of the sebaceous gland, making it squeeze out all its sebum, and, at the same time, making the hair erected[18].

3.2.2 Hair follicle life cycle

The hair follicle too has a life cycle: in fact, it can be divided into two areas, the deepest one that is composed by numerous Keratin cells that proliferate continuously, called the matrix, and the superficial one in which the cells differentiate themselves, the differentiation area. The hair follicle life cycle comprehends three different phases:

- Anagen: it is, in turn, divided in six subphases. In anagen I, the hair follicle cells start to form the bulb which grows towards the dermal papilla and where, in anagen II, it covers it all. The dermal papilla repositions itself away from the bulb and goes deep into the adipose layer. Anagen III is the phase where the bulb, which is not entirely grown yet, starts to form the shaft of the new hair, while in anagen IV all the hair follicles elements are ready, and the shaft of the new hair has reached the follicular collar. The last two phases are the growing related, where the hair's length increases from five to ten times and keeps constant during the whole anagen VI from several weeks to several years[19].
- Catagen: it is a transition phase where the mitotic activity in the matrix of the hair follicle ceases, the vitreous membrane becomes thicker around the bulb, and the melanocytes contract themselves, giving the pigmentation to the hair pili. The lowest part of the follicle is now empty of its cells, and it leaves the dermal papilla uncovered. At this point, all

the cells of the bottom of the follicle assemble and, underneath them, the epidermis forms a structure that maintains them in direct contact with the dermal papilla, forming an epidermal germ that gives start to the regeneration of the hair[14].

- Telogen: once the follicle reaches its minimum length, it enters the last phase of the cycle, the telogen, which lasts three to four months. The dermal papilla is now a little group of cells that places under the epithelial germ[19]. The hair shaft manages to remain inside the follicle thanks to its inferior end, until it gets removed by mechanical stress, like combing, or by the new hair growing in the next anagen, which starts with the change in the dermal papilla output that ignites the process [Fig. 5].

Fig. 5: Hair follicle life cycle; the hair growth starts with the Anagen phase, where the hair follicle cells proliferate vigorously; next there is the Catagen, a steady phase where the cells stop to proliferate, and the hair growth stops. Finally, the Telogen is the quiescent phase where the hair falls and is replaced by a new hair. This picture was taken from[20].

3.2.3 *GLI1*

In one study it was shown that cell-autonomous activation of the Hedgehog pathway, majorly active during the organogenesis, brought to an increase of dermal papilla fibroblast heterogeneity[21]. This induced hair growth hyperactivation and embryonic-like generation of new hair follicles.

Sonic Hedgehog is the main ligand that activates the Hedgehog pathway: it is highly expressed in the keratinocytes of the hair matrix, and it acts as a mitogen factor, developing a signal cascade that ends with the transcription of the effector sequence *GLI1*[21]. *SHH-GLI1* signaling is the responsible for skin development and it is crucial for skin homeostasis. In particular, *GLI1* has a great role in skin regeneration and angiogenesis. It was proven that Sonic Hedgehog, through *GLI1* transcription, induces the transition from a hair follicle telogen to the new anagen[14]. In fact, in the dermal papilla and outer root sheath, there are many *GLI1* cells that stimulate the proliferation and the hair follicle regrowth. Moreover, it was demonstrated that *GLI1* stem cells in mice's hair follicle were higher during the hair follicle growth and decreased after the administration of its inhibitor GANT 61 [22]. Another test on mice displayed that *GLI1* stem cells outside the follicle were clustered in the tissue membrane, and the epidermis and dermis were becoming thicker and thinner respectively, suggesting that *GLI1* plays an important role during the structural changes that happen during skin expansion[22]. *GLI1* stem cells near the perivascular area are fundamental during injury repair and in general to maintain vascular homeostasis. The same study, in fact, their number was clearly increased in the skin if dilated mice, which afterwards migrated and adhered to the outer vessel membrane[22]. *GLI1* cells are also progenitors of vascular remodeling after acute and chronic injuries, thus they could be an interesting target to prevent vascular calcification.

3.3 Basal Cell Carcinoma

Basal Cell Carcinoma (BCC) is the most common type of non-melanoma skin cancer present nowadays: in fact, in the USA it is estimated that there are 2 million new cases each year, with an incidence rate that can go up to 1000/100.000 inhabitants per year, most of which are among Caucasians[23]. This is probably due to the increased exposure to UV light and the tendency of some people to stress the skin using artificial light to have a better tan. Although the number of people diagnosed with this disease has increased dramatically in the

last 30 years, BCC has a low mortality rate because it rarely metastasizes, with an incidence rate that goes from 0.0028 % to 0.55 %[24]. A retrospective evaluation of previous cases from 1981 to 2011 showed that Basal Cell Carcinoma, if metastasizes, occurs for the 53 % in regional lymph nodes, for the 33 % in the lungs and for the 20 % in the bone. It was furtherly seen that between the first tumor appearance and the first metastasis signals 9 years usually pass[24]. Even if it is rare, a recent review displayed that the median survival of distant metastasis of Basal Cell Carcinoma is 24 months, while regional metastasis had a median survival of 87 months[25]. Although there are a few approved drugs in the market, there is still the urge of finding a new pharmacological treatment for patients who resist to these drugs, making them not eligible to surgery. Furthermore, it would allow countries to save money for the Global and National Health Care Systems.

Even if it is one of the most frequent types of skin cancer worldwide, it seems that BCC is not entirely understood after all: it is recognized by little papules or nodules with telangiectasia on the face and the neck, which are the body parts that are most exposed to UV rays, or by superficial lesions that appear to be flat, erythematous, and scaly with demarcated edges, most frequently found on the trunk of young adults; for more advanced tumors we have difficult-to-treat lesions, which have been left without treatment for many years[23]. Patients already affected by other diseases, like Xeroderma Pigmentosum or Basal Cell Naevus Syndrome can develop Basal Cell Carcinoma very early, not reaching 20 years of age[25].

Basal Cell Carcinoma is heterogeneous, it goes from superficial lesions that can be resolved with a small operation to more severe difficult-to-treat lesions. The prognosis is determined by the risk of recurrence of the pathology or its local devastating capacity.

The primary cause of BCC is the excessive activation of Hedgehog pathway, that can derive from a mutation due to long exposure to the sun or artificial light, or from genetic factors: normally, Hedgehog pathway plays an

essential role during vertebrate embryonic development[19], after which, it remains silent, but during tumorigenesis it can be reactivated. Hedgehog pathway is activated mainly by Sonic Hedgehog ligand (*SH*), a protein that binds Patched 1 (*PTCH1*), which normally is bound to Smoothened factor (*SMO*), keeping it inhibited; SH disadvantages this binding, and *PTCH1* releases *SMO*, which activates the cascade signal that increases levels of *GLI1* tumorigenic gene, leading to the decrease of *PTCH1* and to tumorigenesis[26]. Expression of *SUFU*, *SMO*, *PTCH* and *GLI1* seems to be upregulated after skin expansion, with a peak in two or three weeks, and then decreasing. This finds explanation with the importance of Sonic Hedgehog in the Hedgehog pathway, with the effector signal *GLI1* that plays an essential role in the signaling way[22].The activation of the Hedgehog pathway can occur also by inactivating mutations of *PATCH* and activating mutations for *SMO*. These are both majorly induced by UV-rays, and they are related mostly with C-T transitions in the dipyrimidines sites, or they are CC-TT tandem like mutations[25]. Another cause can be the high mutational burden, which implies that second insurgences of Basal Cell Carcinoma can be cured with Immunotherapy.

Basal Cell Carcinoma can be divided into two different subtypes: the first one is the Nodular-like type, which is characterized by roundish areas that do not influence one another. This class of BCC is less dangerous because each area is confined, and it does not tend to spread all over the tissue. The most aggressive BCC is the Infiltrative-like type, a variant that can be recognized by irregular elongated tumor areas, which have the tendency to expand all over the tissue. If untreated, Infiltrative BCC metastasizes, representing a great danger for the patient.

In vitro studies of BCC are limited by the fact that no human BCC cell lines exist, and primary tumor cells do not expand *in vitro*. Indeed, BCC cells can't grow alone and, to survive, they need to maintain their architecture, which is possible only with the stroma cells' help.

3.3.1 Treatments

For the majority of Basal Cell Carcinoma, surgery is still the best treatment, in fact it is used as a standard for nearly all patients. Radiotherapy is also a valid alternative, mostly for elderly patients and in general for those who are not eligible for surgery, as well as those affected by BCC with perineural involvement. However, radiation therapy is not suggested for patients who have genetic predisposition to cancer and connective tissue disease. Retrospective studies showed a comeback from the pathology after 5 years, with rates that go from 4 % to 16 % for patients treated with radiotherapy, while another study on a cohort of 347 patients showed that radiotherapy has a higher level of recurrence (7.5 %) compared to standard excision (0.7 %)[24].

There is no significant result for chemotherapy: the treatment response rate is quite low (20-30 %) but it does not last over than 2-3 months, without mentioning that in elderly patients the adverse effects are quite severe. It is only considered as a second or third-line treatment, in case the Hedgehog inhibitors do not work[25].

A promising approach for Basal Cell Carcinoma is using topical drugs: Imiquimod and 5-fluorouracil are very low-cost drugs that need to be applied twice a day on the tumor area in the treatment of superficial BCC. They are approved by the FDA for treatments that last from three to six weeks, and they showed significant results: a study with 31 superficial BCC patients showed an achievement of 90 % rate after three weeks. Although they bring great results, several adverse effects are associated with this kind of cure, including erythema, pruritic, pain and irritant dermatitis[24].

For difficult-to-treat BCC, Hedgehog inhibitors are requested. This class of drugs targets *SMO*, inhibiting it and avoiding from the start the Hedgehog signaling way, which brings to BCC insurgence. The most utilized approved Hedgehog inhibitors are Sonidegib and, most of all, Vismodegib because it is indicated for both local advanced BCC, for patients who are not eligible for surgery or radiotherapy, and for symptomatic metastatic BCC[27]. Vismodegib is based on a phase II study with a 104-cohort divided in 33 metastatic BCC

patients and 63 locally advanced BCC who all received 150 mg of drug daily. The response was very clear, with a 30 % response in the metastatic and 43 % response in the locally advanced BCC after 7.6 months, with 20.6 % of patients with complete response and 22.2 % with a partial one. These rates increased to 48.5 % for metastatic and 60.3 % for locally advanced BCC after 39 months, with median response times of 14.8 and 26.2 months[28]. The efficacy of Vismodegib is already proven and it is also efficient for preventing the formation of new BCCs. However, after interruption of long-term treatments, there is a relapse of the pathology[29].

Sonidegib is a valid alternative to Vismodegib approved by the FDA for patients not eligible for surgery or radiotherapy and in general for those who have recurrent locally advanced BCC[30]. Its approval comes from the phase II study BOLT, a clinical trial that included metastatic BCC patients unresponsive to conventional therapies. Patients were randomized and subjected to two different drug doses, 200 mg for 79 patients and 800 mg for the other 151. Although results for both doses were similar (43 % for 200 mg Sonidegib compared to 38 % for 800 mg Sonidegib in metastatic patients and 15 % for 200 mg Sonidegib with 17 % for 800 mg in locally advanced BCC patients), the 800 mg Sonidegib displayed severe side-effects after 30 months of follow-up, while 200 mg continued to show promising results, with 56.1 % and 7.7 % of response rate for locally advanced and metastatic Basal Cell Carcinoma, respectively[31].

Both Vismodegib and Sonidegib display several adverse effects, which can be spasms, alopecia, weight loss, fatigue, decreased appetite, diarrhea, nausea, dysgeusia, and ageusia. These conditions make, most of the times, interrupt the therapy for 30 % of the patients. To overcome this inconvenience, little drug holidays are proposed to the patients, to avoid side effects[29].

Sometimes it happens that advanced BCC can resist to Hedgehog inhibitors: in one study 20 % patients were resistant to Vismodegib, while in another one 21 % initially responded to the treatment but became resistant afterwards, reaching an overall 50 % resistance rate, with progression of the

pathology within 54,4 weeks. Finally, one study displayed a 78 % loss of efficacy of Vismodegib after one year of therapy in metastatic BCC patients[24].

4 Aim of the project

In this Master thesis work the aim was to find the optimal culture medium for culturing of tumor explants. To do so, a comparison between M154CF and Co-Culture Medium + EGF has been done, to discriminate which of the two media maintains the best intrinsic characteristics of the tumor after 24 hours of incubation. M154CF is commonly used to culture ASZ-OO1, a murine BCC cell line, while Co-Culture Medium + EGF performs well for short term culture of primary BCC cells.

In this study, tumor explants were collected from three patients to compare the two media. Tumor morphology, proliferation, apoptosis as well as activation of the hedgehog signaling pathway were evaluated to identify the culture medium preserving the best the features of BCC. The markers of the BCC subtypes were also used to identify potential Nodular-to-Infiltrative-like type transitions. Thanks to this work, it will be easier to understand the characteristics of the tumor and it will be possible to do further test with a drug, ensuring that any changes in the BCC explant will be due to the drug itself and not to any other factor.

5 Materials and methods

5.1 Media composition

The two culture media had different compositions: Co-Culture Medium+EGF was constituted by 500 ml of EpiLife (Thermo Scientific, Munich, Germany), a specific medium for the growth of human keratinocytes, Normocin™ (Invivogen, San Diego, CA, USA) with 1 ml/500 ml concentration, which is an antibiotic that prevents cell lines from mycoplasma, bacterial and fungi contaminations, 5 ml/500 ml concentration of Human Keratinocyte Growth Complement (Creative Biolabs, Shirley, NY, USA), and 0.01 µg/ml of Epidermal Growth Factor (Merck, Readington, NJ, USA), a small protein that assists in promoting skin health by inducing cellular division and protein synthesis, reducing any sign of aging.

M154CF instead is composed by M154CF medium (Gibco™ by Life Technologies, Grand Island, NY, USA), 2 % of chelexed FBS (Gibco™ by Life Technologies, Grand Island, NY, USA) to give the nutrients to the cells, 1 % of PenStrep (Thermo Scientific, Munich, Germany), an antibiotic to avoid external contaminations, and 150 µl/500 ml of $CaCl_2$ (Merck, Readington, NJ, USA) in M154CF medium: Calcium is fundamental to induce differentiation to the keratinocytes, stimulating their growth.

5.2 Sample treatment

Tumor explants were taken directly from the hospital and brought to the laboratory, where they were decontaminated under biological hood (SafeFAST Premium, Faster, Ferrara, FE, Italy) with a solution 1 % of Gentamicin/Amphotericin B (Gibco™ by Life Technologies, Grand Island, NY, USA) in PBS buffer (Laboratorium Dr. G. Bichsel AG, Interlaken). Then, they were cut with little blades in pieces of 4-6 mm of diameter, and put in a 12-well-plate (Falcon®, Corning Incorporated, NY, USA), one piece in 1 ml solution of Co-Culture Medium+EGF, and the other in 1 ml solution of M154CF.

The explants were put in the incubator (Galaxy 170 S, New Brunswick, USA) for 24 hours at 37° C, and the next day were put for 4-6 hours in a solution of Formalin 4 % in Phosphate Buffer (Biosystems AG, Muttenz, Switzerland) to fix the samples, and stored in a solution of Ethanol 70 % afterwards (Reactolab, Servion, Switzerland). The explants were then placed in the tissue processor (Shandon Citadel 2000, Portsmouth, NH, USA) for more than 19 hours, following these steps; 1 h 20 Alcohol 70 %, 1 h Alcohol 95 %, 1 h Alcohol 95 %, 1 h 20 Alcohol 95 %, 1 h Alcohol 100 %, 1 h 20 Alcohol 100 %, 2 h Alcohol 100 %, 2 h Alcohol 100 %, 1 h 20 Xylene, 2 h Xylene, 2 h Paraffin, 3 h Paraffin. The tissues were then included in paraffin blocks and placed at -20° C for solidification. Paraffinized samples were cut in 5 μm tissue sections at the microtome (Microm HM 325, Epredia™, Portsmouth, NH, USA); after that, they were placed on a warm bath at 37° C (HIR-3, Axel Johnson Lab System, New York, NY, USA), taken up with a microscope slide (Superfrostand, Epredia™, Portsmouth, NH, USA) and placed in the fridge at 5° C (Liebherr ProfiLine, Switzerland) for 24 hours. The next day the samples were tested with the chosen assay and later placed again in the fridge at 5° C overnight. Finally, they were analyzed at the scanner to get the final images [Fig. 6].

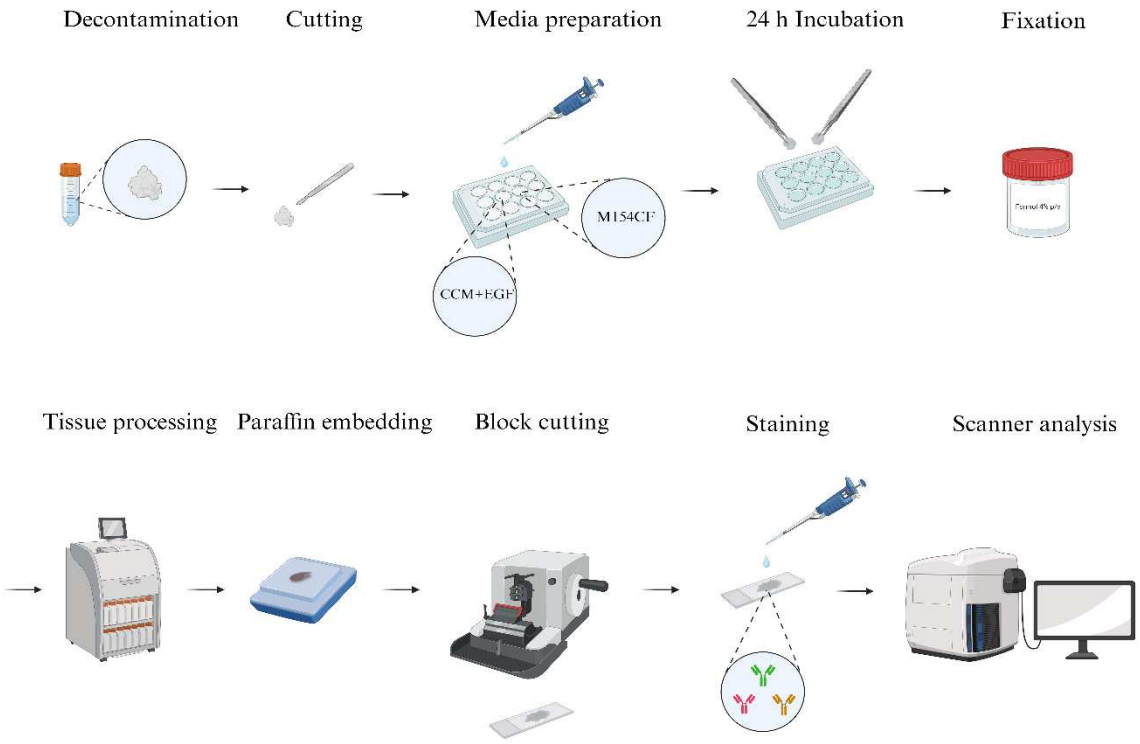

Fig. 6: Work process; the samples were decontaminated, cut and incubated, then tested after fixation and paraffinization with paraffin blocks. Each tissue was eventually analyzed at the scanner, obtaining an image that emphasized the markers of interest.

5.3 Hematoxylin & Eosin staining

This staining is fundamental to see the morphology and architecture of the tissue and the tumor areas: based on this, it is possible to see how the tumor and stroma cells are organized and recognize which type of skin cancer is at hand.

Samples were taken out from the fridge and placed on a heat plate (Digital Heat Block, Benchmark Scientific, NJ, USA) for 10 minutes at 56° C. After that, they were treated under chemical hood (LUSODUR®, Casale sul Sile, TV, Italy) with the following solutions: 3 minutes Xylene (Reactolab, Servion, Switzerland), 3 minutes Xylene, 3 minutes Alcohol 100% (Reactolab, Servion, Switzerland), 3 minutes Alcohol 100 %, 3 minutes Alcohol 95 % (Reactolab, Servion, Switzerland), 3 minutes Alcohol 70 % (Reactolab, Servion, Switzerland), 3 minutes Distilled Water. This was done to rehydrate the tissue by

decreasing the percentage of alcohol gradually. Out of the hood, the samples were put twice in PBS for 5 minutes. Later, the explants were placed in a beaker full of tap water for 15 seconds, and then put in a Harris Hematoxylin solution for 2 minutes: Hematoxylin dyes basophilic components, therefore it enlightens the nuclei and the cytoplasm, cell compartments that are crammed with nucleic acids[32].

The samples were then placed in a new glass of tap water for other 15 seconds and put in and out an Alcohol/acid solution for 5 times to wash away the excessive Hematoxylin; after that, they were placed in another glass of water with a small thread drop continuously falling from the tap for 4 minutes, and, later, the tissues went in and out an Eosin solution for 7 times: unlike Hematoxylin, Eosin dyes acidophilic structures, like the Extracellular Matrix, blood cells and part of the cytoplasm, which are areas lacking of nucleic acids[32].

Quickly, the samples were placed under the chemical hood, following these steps: 2 minutes Distilled Water, 2 minutes Alcohol 70 %, 2 minutes Alcohol 95 %, 2 minutes Alcohol 100 %, 2 minutes Alcohol 100 %, 2 minutes Xylene, 2 minutes Xylene. This process was done to rehydrate the samples. The ultimate tissues were finally treated with two drops of Eukitt medium (ORSAtec, Bobingen, Germany), covered with Microscope cover glasses and placed at 5° C for 24 hours. The next day they were analyzed at the scanner (Ventana DP 200, USA).

5.4 Proliferation and Apoptosis Immunofluorescence staining

The goal is to emphasize two biomarkers for proliferation and apoptosis (MKI67 and Cleaved-Caspase 3) to understand if the tumor has changed its characteristics in one of the two media. To do so, primary antibodies targeting MKI67 and Cleaved-Caspase-3 bind to these cells expressing proteins specifically; the resulting binomial is then recognized by a fluorescently-labelled secondary antibodies solution which binds it; the final antigen-antibody complex

can be enlightened by the fluorescent lamp and show the proliferating and apoptotic cells[33].

Samples were placed on a heat plate (Digital Heat Block, Benchmark Scientific, NJ, USA) for 10 minutes at 56° C. After that, they were treated under chemical hood with the following solutions: 3 minutes Xylene, 3 minutes Xylene, 3 minutes Alcohol 100 %, 3 minutes Alcohol 100 %, 3 minutes Alcohol 95 %, 3 minutes Alcohol 70 %, 3 minutes Distilled Water. Out of the hood, the slides were placed twice in PBS for 5 minutes. In the meantime, a rice cooker (IHC WORLD, Ellicott City, MD, USA) was filled with distilled water and prewarmed for 20 minutes, with a case full of Antigen Retrieval solution within it. (Invitrogen, Waltham, MA, USA)[34]. Once the explants had finished their second 5 minutes in the PBS solution, they were inserted into the Antigen Retrieval case and placed inside the rice cooker for 20 minutes: the Antigen Retrieval contains Sodium citrate (10 mM, pH), EDTA (1 mM, pH 8) and Tris/EDTA (pH 9) buffers; this solution reactivates the epitopes, that momentarily are still fixed, to let the biomarkers interact with the Primary Antibody. After this time, the rice cooker was switched off and the solution with the tissues inside was put to rest inside for another 20 minutes time.

During this 40-minute window, the Primary Antibody Solution was prepared: for proliferation the mouse derived antibody for Pan cytokeratin Lu5 (1:500, Invitrogen, Waltham, MA, USA) was used to see the keratinocytes, and the rat derived antibody for MKI67 SolA15 (1:300, Invitrogen, Waltham, MA, USA) was the responsible for proliferation signal; for what concerns apoptosis, instead, alongside the antibody for Pan cytokeratin, it was used the polyclonal rabbit anti-human for Cleaved Caspase-3 (Asp175, 1:200, Cell Signaling technology, Danvers, MA, USA). For both stains DAKO (Agilent Technologies, Santa Clara, CA, USA) was needed as diluent for the antibodies.

After the 40 minutes, the slides were taken out and washed fast with PBS, then placed other two times of 5 minutes each in other PBS; later, the samples were put in a solution of Triton-x100 0.012 % in PBS for 30 seconds, and, after

that, washed in PBS and placed for other two 5-minute time in other PBS: Triton-x100 0.012 % lets the cells' membranes become more permeable without denaturing the proteins, so that later the antibodies can penetrate within the cells.

Excess of liquid was then removed from the slides and tissue sections were surrounded with a PapPen. The slides were placed in a humidified incubation chamber. Consequently, 70 µl of the Primary Antibody Solution were dropped on each tissue section; once each sample was covered with the antibody solution, the chamber was closed, and the tissues were let to rest for 2 hours. Afterwards, the slides were washed with PBS fast and then placed for 5 minutes in a PBS solution + 0.05 % Tween, which binds all the non-specific sites of the protein that could give background signals.

In the meantime, Secondary Antibody Solution was prepared: using always DAKO as antibody diluent, for proliferation a goat anti-mouse antibody labeled with AF488 dye was used for Lu5 primary antibody, while a donkey anti-rat antibody labeled with AF555 dye for the MKI67 one (Invitrogen, Waltham, MA, USA); for apoptosis, instead, polyclonal anti-rabbit IgG (H+L) antibody fluorescently-labeled with AF546 dye (Invitrogen, Waltham, MA, USA) was needed. All the secondary antibodies were diluted by 1:500 and the final solution was protected by light because the fluorophore is sensible to it.

After the PBST solution, the samples were washed fast with PBS and then in other PBS solution for 5 minutes. After the slides were dried around the tissue as before, they were placed back in the incubation chamber and 70 µl of Secondary Antibody Solution were dropped until full cover of the sample area. The slides were then put to rest for 30 minutes in the dark to avoid photobleaching of the fluorescent dye. Later, the samples were washed fast with PBS and then another time with other PBS for 5 minutes in the dark. After that, another 5 minutes with PBST were necessary, then fast with PBS and one last time for 5 minutes in PBS. All these operations were performed in the dark. Finally, the slides were dried, and 40 µl of mounting medium containing DAPI was dropped (Invitrogen, Waltham, MA, USA). Each sample was covered with

microscope glass, and then placed in the fridge at 5° C for 24 hours. DAPI emphasizes the nuclei. The next day the samples were analyzed at the scanner and the fluorescent lamp. The data collected were utilized to calculate two different quantities: the first one was the proportion of proliferating/apoptotic cells over the total number of tumor cells within six different areas arbitrarily chosen inside each tissue. To do so, every tissue was visualized on SlideViewer program (3DHISTECH, Budapest, Hungary) and every cancerous cell in the selected areas was counted; next, the cancerous cells expressing the biomarker were counted and the following ratio was done:

$$Proportion\ of\ proliferating/apoptotic\ cells: \frac{n\ proliferating/apoptotic\ cells}{total\ n\ cancerous\ cells} \times 100$$

Each result for each area was collected and plotted on a histogram comparing the two culture media, using the GraphPad Prism software (Dotmatics, Bishop's Stortford, United Kingdom). The second quantity analyzed was the Mean pixel intensity of each biomarker in each cell inside the selected areas. To measure these values, two different screenshots of the same picture were made in the SlideViewer program: the first one depicted the tumor area selected and the second one only the biomarker signal. Using the first picture, the edges of each cell were drawn using the Fiji app program (National Institute of Health, Bethesda, USA), to recognize them later. Furtherly, the drawn cells were juxtaposed with the biomarker image and then for each polygon it was measured the Mean pixel intensity inside it. Lastly, the values collected were plotted on a histogram on GraphPad Prism and compared, enlightening the results strength calculating the R^2 value via an unpaired t test.

5.5 Fluorescent In Situ Hybridization stains (FISH)

FISH staining combined with immunofluorescent staining furnishes two different signals at the same time, the protein one, with which it is possible with an antibody to detect Pan cytokeratin signal for keratinocytes, and the mRNA one with FISH probes[35].

For the comparison of the two culture media, two different FISH stains were performed: the first one helped to recognize *GLI1,* highlighting activation of the Hedgehog pathway, and *SPON2* signals; *GLI1* is activated for the organogenesis of most mammals organs and then silenced; a reactivation of the pathway might happen for onsets of cancers, and it can be visible for the increased expression of *GLI1*, last passage of the effector cascade process. *GLI1* is also expressed in normal skin cells at hair follicle level, in fact it might be confused for its presence; *SPON2* is a cell adhesion protein that promotes adhesion and outgrowth of hippocampal embryonic neurons; it is also essential in the initiation of the innate immune response and represents a unique pattern-recognition molecule in the extracellular matrix for microbial pathogens[36]. Although it has not be proved yet its influence in BCC study, it was observed that in BCC areas there is a great expression of this mRNA sequence. By the presence of both *GLI1* and *SPON2* signal it becomes clearer if the portion of sample analyzed is a healthy or a cancerous area.

For the second type of FISH staining, a deep look into the tumor differentiation is made: as seen before, there are mainly two different kinds of BCC: the first one is Nodular-BCC, a less aggressive type of cancer characterized by roundish delimited areas that do not interfere one another and stay still within the tissue; on the other hand, there is Infiltrative-BCC, which is represented by elongated cancerous areas that tend to spread all over the tissue, trying to metastasize. However, there is a chance that Nodular-BCC can turn into Infiltrative-BCC with time. For this reason, this FISH is meant to understand if there is this degeneration and if so at which point: to investigate this, *MPPED1* and *KRT6A* are used as markers at mRNA level; *MPPED1* is a biomarker that is

present most of all into Nodular-BCC areas, while *KRT6A* is expected to be found in Infiltrative-BCC. The aim is to find areas with both signals and understand if there is a correlation between the two markers expression.

Co-Detection Target Retrieval 1x was placed in a small case, and the whole of it in the rice-cooker to warm up. This solution is meant to render epitopes and mRNA molecules accessible for the staining process. The slides were placed on the heat plate at 56° C for 10 minutes, then, as in the previous protocols, they were placed under the chemical hood in the following solutions: 3 minutes Xylene, 3 minutes Xylene, 3 minutes Alcohol 100 %, 3 minutes Alcohol 100 %, 3 minutes Alcohol 95 %, 3 minutes Alcohol 70 %, 3 minutes Distilled Water. Afterwards, the slides were dried all around the tissue and then 2-3 drops of H_2O_2 (Advanced Cell Diagnostics, Newark, CA, USA) to cover the entire sample area, and let to rest for 10 minutes. The samples were immersed two times for 3 minutes in a distilled water solution and then placed in the case with Co-Detection Target Retrieval inside the rice-cooker for 15 minutes.

In the meantime, the Primary Antibody Solution was prepared: Lu5 diluted in Co-Detection Antibody Diluent (1:250) was used as primary antibody to detect keratinocytes.

After the rice-cooker, the hot slides were transferred immediately to a distilled water solution and then washed other two times for 2 minutes. Afterwards, the samples were washed for 2 minutes in a PBST (PBS+0.1 % Tween at pH 7.2-7.4) and later dried and placed in an incubation chamber where 65 µl of Primary Antibody Solution were added. The incubation chamber was then closed and the slides within it were put at rest for two hours at room temperature; in the meantime, a humidified box was placed inside the oven at 40.6° C (UN 55, Memmert, Buchenbach, Germany). Later, the antibody solution was washed away from the slides two times for 2 minutes in PBST, and then, under chemical hood, they were immerged in a Zinc buffer Formalin solution (Thermo Scientific, Munich, Germany) for 30 minutes at room temperature; this solution is meant to fix the antibody on the tissue.

Meanwhile, *GLI1*-C2, *SPON2*-C1 reagents (*KRT6A*-C2 and *MPPED1*-C1 for second type FISH, Advanced Cell Diagnostics, Newark, CA, USA) and the Wash Buffer were warmed up at 40.6° C for 10 minutes to avoid that their precipitation later, and then let to rest until need, while the 1x Wash Buffer was prepared, diluting warmed 50x Wash Buffer in distilled water.

After the Zinc buffer Formalin, the slides were washed for 2 minutes in PBST under the hood and then other two times outside it. The prewarmed humidified staining box was taken out of the oven the slides placed on it after drying them all around the tissue area; consequently, 1-2 drops of Protease Plus Reagent were added to help the probes penetrate and link better to the mRNA. Later, the slides inside the humidified box were incubated in the oven at 40.6° C for 30 minutes. The tissues were washed two times for 2 minutes in distilled water, while the humidified box was placed again inside the oven to maintain its temperature.

Meanwhile, the probe solution was prepared: *SPON2*-C1 or *MPPED1*-C1 are ready to use solutions that can be used for the C2 channel. Here, *GLI1*-C2 was diluted 1:50 in *SPON2*-C1, while *KRT6A*-C2 was diluted 1:100 in *MPPED1*-C1. The slides were removed of the excess of liquid they have around the sample, and then they were placed inside the humidified box. 1-2 drops of the appropriate mix were added and later the slides were placed in the oven within the box for 2 hours at 46° C. After this time, the tissues were washed three times for 3 minutes in 1x Wash Buffer and finally stored in 5x SSC (buffer to conserve the samples) overnight at room temperature.

The next day, AMP-1, AMP-2, AMP-3, HRP-C1, HRP-C2, HRP-C3 and HRP-blocker solutions were placed at room temperature for at least 30 minutes (Advanced Cell Diagnostics, Newark, CA, USA); in the meantime, the slides were washed two times for 2 minutes in the 1x Wash Buffer. After having removed the excess of liquid, they were placed in the prewarmed humidified staining box[37], and 1-2 drops of AMP-1 were added to cover the tissue area (Advanced Cell Diagnostics, Newark, CA, USA). The box was then placed for

30 minutes in the oven at 40,6° C. The samples were washed three times for 3 minutes in 1x Wash Buffer, while the humidified box was placed again in the oven to keep its temperature. Another time, the excess of liquid was removed, and the slides moved within the staining box, where 1-2 drops of AMP-2 (Advanced Cell Diagnostics, Newark, CA, USA) were falling on the tissue surface. The humidified box was closed and then put in the oven once more at 40.6° C for 15 minutes. The samples were washed a third time for three times of 3 minutes each with 1x Wash Buffer, as the humidified box was kept warm in the oven. Consequently, the excess of liquid was removed again from the slides, which were placed in the humidified box and added of 1-2 drops of AMP-3 (Advanced Cell Diagnostics, Newark, CA, USA) and the whole package was put once again in the oven for 15 minutes at 40.6° C. Afterwards, the samples were washed other three times of 3 minutes each, as the staining box was kept in the oven. After having removed the excess of liquid, the tissues were placed back in the oven and were covered with 1-2 drops of HRP-C1 (Advanced Cell Diagnostics, Newark, CA, USA), then they were incubated in the oven inside the staining box for 15 minutes at 40.6° C. During this repeated-step process, the hybridized probe-mRNA sequences are amplified multiple times to emphasize the mRNA signal. Imagining the probes like two Z of 14 base pairs each, on one end they hybridize with the mRNA, on the other end, instead, they bind to the pre-hybridization complex, which links the amplifiers, responsible of the increase of the mRNA signal [Fig. 7].

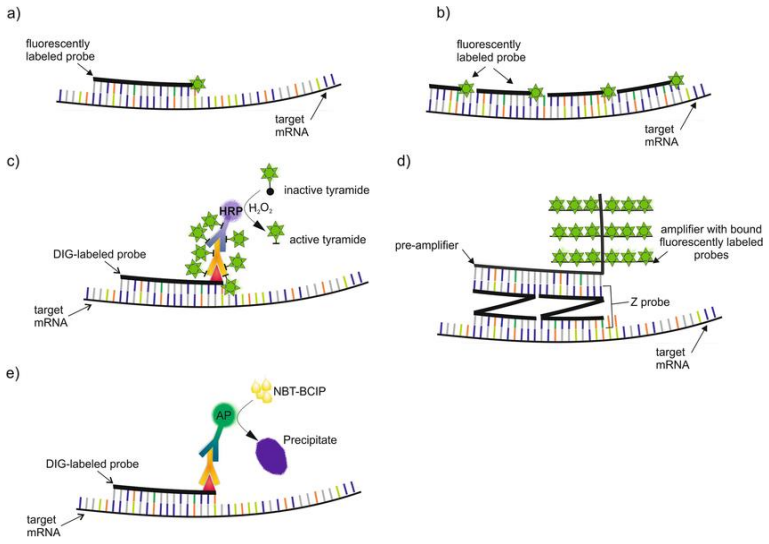

Fig. 7: Amplification of hybridized probe-mRNA sequences; the Z-structured probes manage to hybridize the mRNA on one end, while with the other they link to the pre-hybridization complex. The resulting structure then links to the amplifiers, which increase the mRNA signal and, after interaction with the fluorescent dyes, will make the signal visible under fluorescent lamp. This picture was taken from[38].

After the amplification was done, HRP-C1 was attached to make the whole compound recognizable by the fluorescent markers. During these last 15 minutes, the OPAL fluorophores were prepared: OPAL 570 (Advanced Cell Diagnostics, Newark, CA, USA), which gives a red signal, was used to enlighten *SPON2* or *MPPED1* for the transition FISH (1:1500), while OPAL 650 (Advanced Cell Diagnostics, Newark, CA, USA), which gives an orange signal, was used for *GLI1* or *KRT6A* (1:1500). The slides were washed three times for 3 minutes in 1x Wash Buffer, while the humidified staining box was placed back in the oven. After having removed the excess of liquid, the samples were placed once more in the staining box, added of 65 µl of OPAL solution, and let to rest in the oven for 30 minutes at 40.6° C. Afterwards, the slides were washed for a 3-minute time three times in 1x Wash Buffer in the dark because the OPAL degrades very easily with light, while the humidified box was still put in the oven. The excess of liquid is then removed from the slides, which are next positioned in the humidified box and added of 1-2 drops of HRP-blocker (Advanced Cell Diagnostics, Newark, CA, USA), that terminates the interaction between HRP-C1 and OPAL. The box was closed and placed again in the oven

for 15 minutes at 40.6° C. Subsequently, the slides were washed three times for 3 minutes in 1x Wash Buffer, always in the dark, while the humidified staining box was moved once more in the oven. Removed the excess of liquid, the samples were covered with 1-2 drops of HRP-C2 (Advanced Cell Diagnostics, Newark, CA, USA) and placed back inside the oven within the staining box for 15 minutes at 40.6° C. As for the previous passages, after washing three times with 1x Wash Buffer and having removed the excess of liquid, 1-2 drops of the second OPAL covered the tissues and, after another 30-minute cycle at 40.6° C in the oven and three times wash, the HRP-blocker was added to stop the interaction between the HRP-C2 and the fluorescent marker. The slides were then placed for the last time in the warmed humidified staining box and placed in the oven for 15 minutes at 40.6° C. During the next 3 minutes three times wash, the Secondary Antibody Solution was prepared, using goat-anti mouse AF488 antibody for Lu5, diluted in Co-Detection Antibody Diluent (1:500, Advanced Cell Diagnostics, Newark, CA, USA). After the excess of liquid was removed, the tissues were placed in the incubation box and added of 65 µl of Secondary Antibody Solution that covered the entire sample area. The slides were then incubated for 30 minutes at room temperature, which next followed a two-time wash with PBST solution of 2 minutes each. When the excess of liquid was removed, the samples were let slightly drying and, afterwards, 20 µl of mounting medium with DAPI was added, and the glasses were covered with a coverslip. The slides were let to dry once again for 30 minutes at room temperature and finally placed in the fridge at 5° C overnight. The next day they were analyzed at the scanner and the fluorescent lamp to get the results. With the data collected, the Mean pixel intensity of each biomarker signal was calculated using SlideViewer and Fijiapp programs, and the results were plotted on a histogram using GraphPad Prism alongside the R^2 value. Later, the two pairs of biomarkers were plotted on a XY graph to see the correlation between *SPON2* and *GLI1* and between *MPPED1* and *KRT6A*, emphasizing the level of correlation with the calculation of the straight-line equation. The proportion of biomarker expressing cells calculations were not relevant for these kinds of staining.

6 Results

Three different patients were analyzed to understand better BCC structure and behavior: all these patients have different characteristics which gave us a bigger overview of the pathology and, at the same time, made us catalog the multiple scenarios that were encountered.

Unfortunately, some stains did not give an acceptable result and were not considered during this work.

6.1 Patient 1

6.1.1 Hematoxylin-Eosin staining

Patient 1 was the classic example of a subject affected by Nodular-BCC: as the Hematoxylin-Eosin (H&E) staining shows in [Fig. 8], this type of tumor displays many roundish tumor areas: although they are numerous and can grow, they do not spread around the tissue or assemble, on the contrary, the cells remain isolated and circumscribed, making it difficult for them to metastasize. These characteristics make Nodular-BCC less dangerous compared to the Infiltrative-like type.

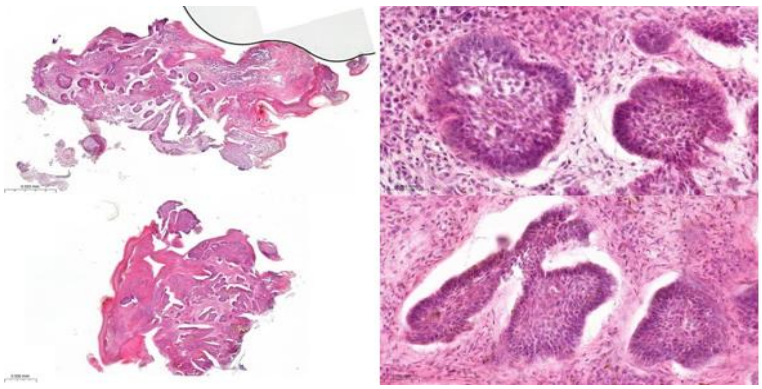

Fig. 8: Patient 1, Hematoxylin-Eosin staining; both CCM+EGF and M154CF display numerous spot-like tumor areas. Cells arrange themselves forming neoplastic circles that do not affect the others around.

Both CCM+EGF and M154CF enlighten this peculiar structure of the tumor, and it seems that neither of the two culture media influence its structure and stroma area, necessary to maintain the tumor structure and thus the tumor integrity. Even after the comparison with the H&E staining of the same sample right after its excision from the patient, we do not see differences ([Fig. 9]).

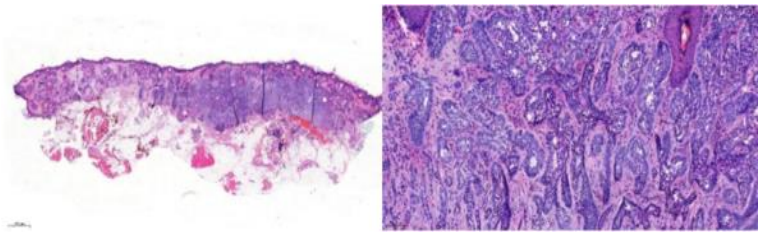

Fig. 9: Patient 1, Hematoxylin-Eosin test of the tissue right after the exportation from the patient. The roundish areas confirm the Nodular-like type of the tumor.

6.1.2 Proliferation Immunofluorescence staining

For proliferation, two different data sets were collected within six selected areas: the first one deals with the number of cells that proliferate within a cancerous area compared to the total number of keratinocytes inside that same area, the second one, instead, consists of how much intense the proliferation signal for each cell; with both these information, it will be possible to take a look to how fast the cancer cells are still dividing in culture.

Patient 1 here shows a great level of proliferation: in the next images, the nuclei of the cells are enlightened with DAPI in blue, while, thanks to Pan cytokeratin (PANCK), the keratinocytes signal can be seen in green ([Fig. 10 a., c., e., g.]); PANCK is a mixture of two or more antibodies that detect high amounts of Keratin. Consequently, it is a great marker for the detection of keratinocytes in general, and they are largely utilized for the neoplastic stains[39]. Finally, the red signal, given by the MKI67, allows to recognize the proliferating cells ([Fig. 10 b., d., f., h.]); within all the tumor areas, the proliferating activity

in patient 1 is quite high, with a remarkable lead by M154CF in both number of cells and intensity of proliferation.

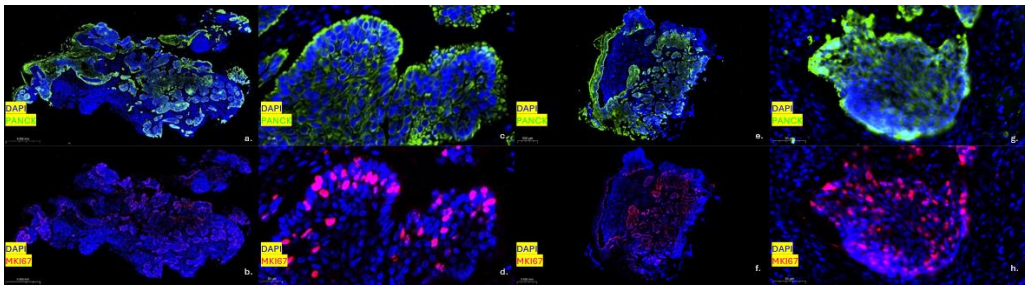

Fig. 10: Patient 1, Immunofluorescence Proliferation staining; Pan cytokeratin signal emphasizes in green the keratinocytes, enlightening the tumor areas (a., c., e., g.). The red signal corresponds to MKI67, which shows the high proliferating activity (b., d., f., h.). Proliferation seems to be highly active in both CCM+EGF (a., b., c., d.) and M154CF (b., d., f., h.).

As [Fig. 11] shows, the proliferating rate of all the selected areas in M154CF overtakes 60 %, while for CCM+EGF is only above 40 %; a similar proposition can be done for the intensity, where M154CF scores around 30 Mean pixel intensity and CCM+EGF does not even reach 20.

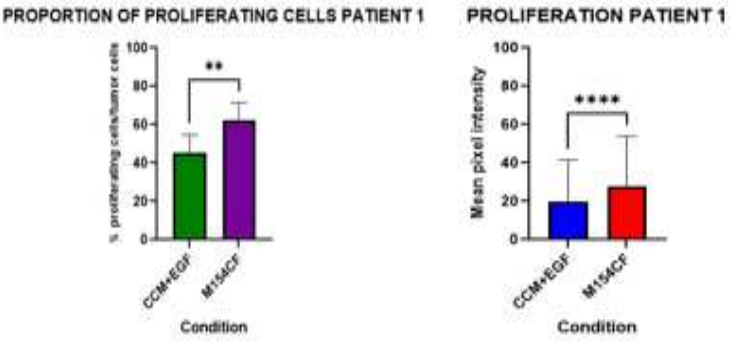

Fig. 11: Patient 1, proportion of proliferating cells (left) and mean pixel intensity of proliferation (right); in both tests M154CF has a higher score.

6.1.3 Apoptosis Immunofluorescence staining

For what concerns Apoptosis, the situation is different: here the red signal represents Cleaved-Caspase 3 staining that shows dying cells. In patient 1 the Apoptosis signal is visibly lower than the proliferation one in both culture media, with only a few cells that express it and with not so much strength, as shown from [Fig. 12].

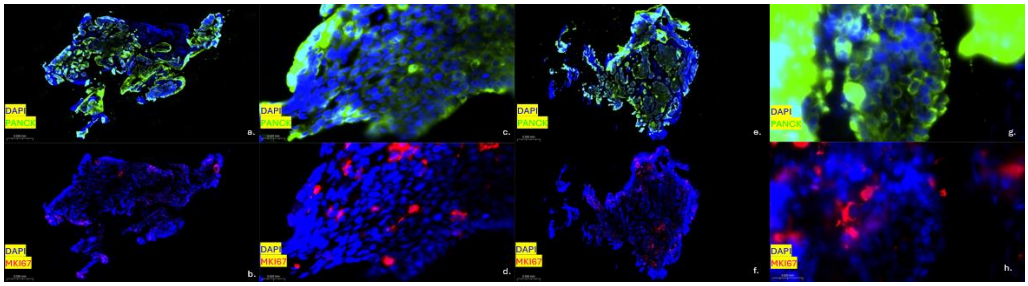

Fig. 12: Patient 1, Immunofluorescence Apoptosis staining; both CCM+EGF (a., b., c., d.) and M154CF (e., f., g, h.) seem to have a lower expression of Cleaved-Caspase 3 compared to the Proliferation staining.

These results are hopeful because the numbers are extremely low: as [Fig. 13] tells, CCM+EGF has the highest score for number of apoptotic cells, but compared to the proliferation data is half, while M154CF is even less than one third; for intensity, instead, both culture media cannot reach 5 % score. The conclusions made are that apoptosis has a very low rate after a 24-hour incubation. However, it is not clear whether the low apoptosis rate is real or due to a defect in the staining protocol. Thus, a longer incubation time was used to try to increase the apoptosis rate and validate the staining quality.

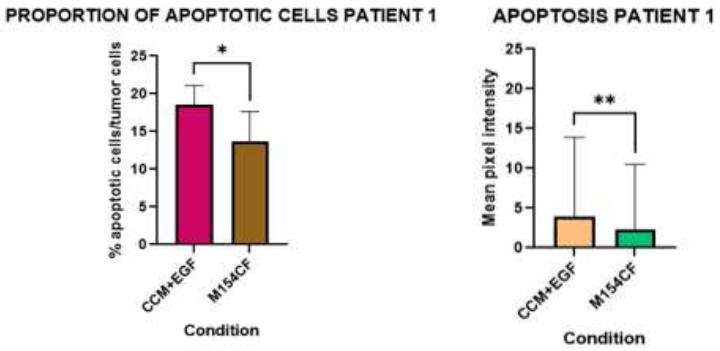

Fig. 13: Patient 1, Proportion of Apoptotic cells (left) and Mean Pixel intensity calculation (right); CCM+EGF has higher values in both graphs, however they are much lower compared to those of the proliferation test.

6.1.4 SPON2-GLI1 FISH staining

The first FISH staining of *GLI1* (orange) was meant to check for maintenance of Hedgehog pathway activation during tissue culture ([Fig. 14 b., d., f., h.]), whereas *SPON2* staining (red), a mRNA sequence that is still to be proven being correlated with BCC ([Fig. 14 a., c., e., g.]) was performed in parallel. In fact, it was observed that in tissues with BCC, the cancerous areas highly express *SPON2*, thus it was considered to better recognize the tumor. Therefore, both signals were expected to be high in both culture media and averagely this is the case for patient 1: the signals are very present throughout the whole tissue, with a particular concentration inside the tumor area of both mRNA sequences.

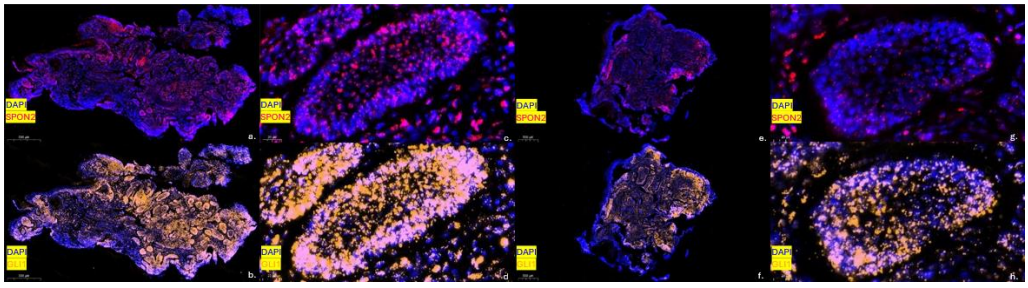

Fig. 14: Patient 1, SPON2-GLI1 FISH staining; both biomarkers seem to be spread all over the tissue and intense in both media; SPON2, in red, (a., c., e., g.) seems to respond well to the test; GLI1, in orange, (b., d., f., h.) seems to have more intense values within the tumor areas.

GLI1 has a better expression in CCM+EGF while in CCM+EGF it reaches 40 %, while *SPON2* is majorly represented by CCM+EGF and for M154CF is only 10 %, as [Fig. 15] shows. The overlapping of these two signals, with the Pan cytokeratin signal help, confirms the identity each of the tumor areas within patient 1 tissue. To confirm this last observation, both *SPON2* and *GLI1* were plotted to see the correlation between the two signals within the tumor tissue; it comes out that there is a positive correlation in both culture media, with a straight line that evidently goes up, as indicated below.

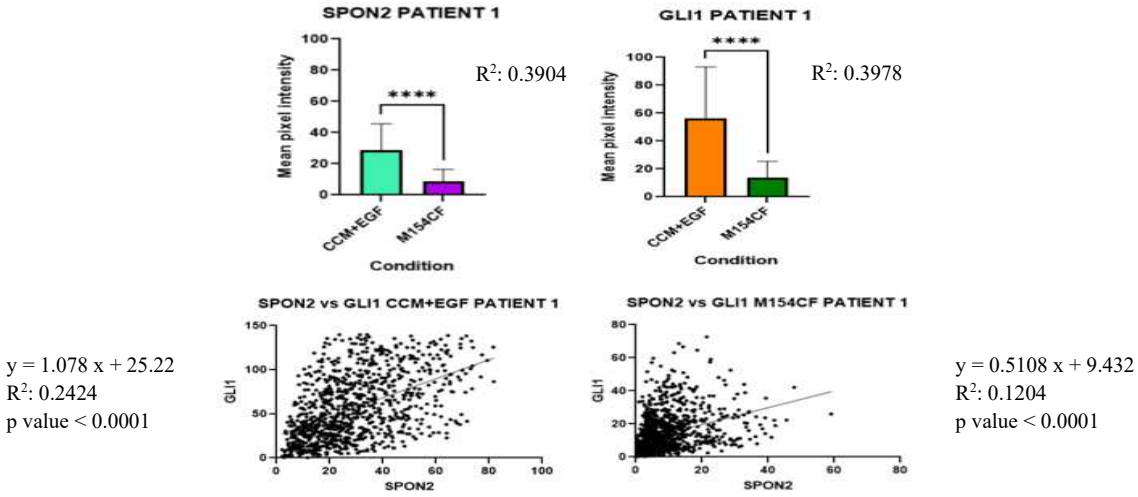

Fig. 15: Patient 1, SPON2 and GLI1 Mean intensities (top left and right) and biomarker's correlation (low left and right); CCM+EGF is significantly higher in both tests, although even M154CF score is remarkable in the GLI1 assay; correlations in both culture media (low left and right) show a positive trend.

6.1.5 MPPED1-KRT6A FISH staining

For the transition FISH, the aim is to try to understand if there is a transition from the less aggressive Nodular-BCC to the more dangerous one Infiltrative-BCC: in fact, despite one patient exhibits Nodular-BCC characteristics, it may be possible that these get to worse and become to show Infiltrative-BCC peculiarities, which are more severe and if not treated could

bring to metastasis. This study tries to find if with the tumor explants it is possible to recognize the transition between the two cancerous forms.

To detect signals of both Nodular and Infiltrative BCC, two different biomarkers were exploited: the first is *MPPED1*, a mRNA sequence visible in red that is expressed mainly in Nodular-BCC ([Fig. 16 a., c., e., g.]), the second one is *KRT6A*, an orange marker that, on the contrary, is mainly associated with Infiltrative BCC ([Fig. 16 b., d., f., h.]).

In patient 1, *MPPED1* was obviously the most expressed one, with a few areas with both signals; the focus of this study was to discover if there were areas with both *MPPED1* and *KRT6A* signals and, if so, to determine if there is a transition from Nodular-like BCC to Infiltrative-like BCC.

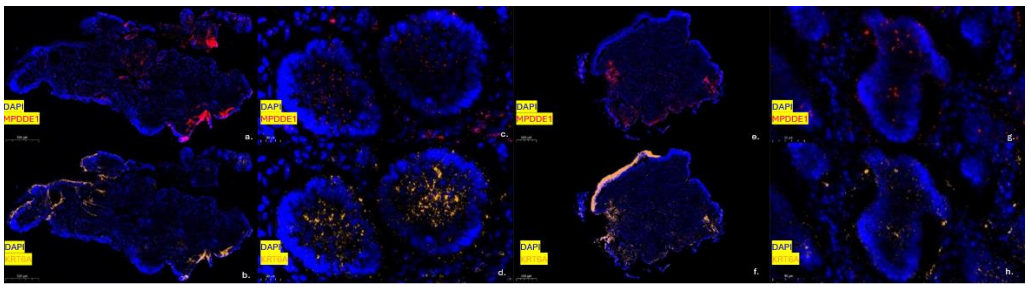

Fig. 16: Patient1, MPPED1-KRT6A FISH staining; MPPED1, in red, (a., c., e., g.) seems to have low values in both media, as well as KRT6A, in orange, (b., d., f., h.), but the staining may display some correlation and therefore a Nodular-Infiltrative like transition.

In general, the signal scores are not quite high and there is a slight difference between the two biomarkers: in fact, as shown in [Fig. 17], for *MPPED1* the signal intensity is higher in M154CF compared to CCM+EGF; on the other hand, despite *KRT6A* is more present in the whole M154CF tissue, there is a greater intensity in the CCM+EGF shared areas. Nevertheless, the presence of both *MPPED1* and *KRT6A* in the same tumor zones could be a proof of the transition from Nodular to Infiltrative BCC, as demonstrated below, where it can be seen a positive correlation between the two signals in both CCM+EGF and M154CF, as the straight lines show. The ideal situation would be to have a

negative correlation, with high *MPPED1*^{high} *KRT6A*^{low} highlighting the nodular extremity and *MPPED1*^{low} *KRT6*A^{high} highlighting the infiltrative extremity of the transition.

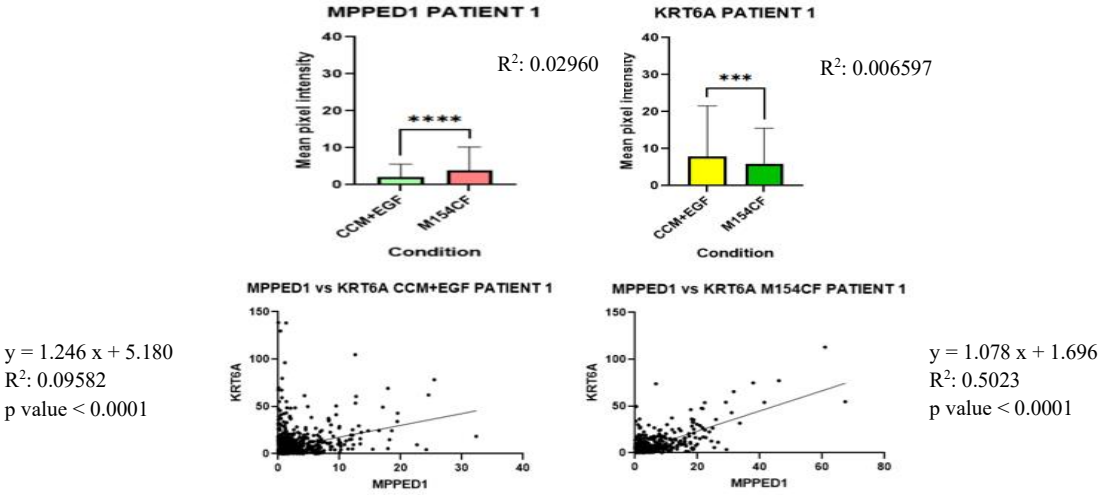

Fig. 17: Patient 1, MPPED1 and KRT6A Mean pixel intensities (top left and right) and biomarker's correlation (low left and right); M154CF shows a higher score in the MPPED1 calculation; on the contrary, CCM+EGF has a higher score for KRT6A, which suggests a higher tendency to pass from Nodular-BCC to the Infiltrative-type. Both media show a positive correlation between both biomarkers.

6.2 Patient 2

6.2.1 Hematoxylin-Eosin staining

The second patient is completely different from the first one: unlike patient one in fact, it discloses a typical Infiltrative-BCC pattern. As [Fig. 18] illustrates, this kind of tumor does not have any isolated areas like the Nodular type but, instead, it is characterized by irregular elongated tumor segments that tend to spread all over the tissue area, with the tendency of influencing the nearby tissues or organs.

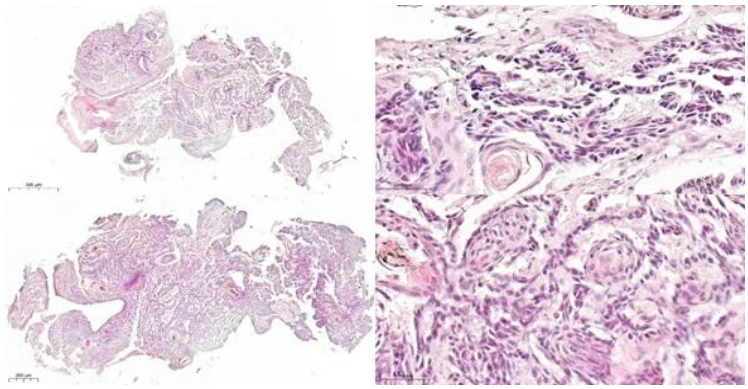

Fig. 18: Patient 2, Hematoxylin-Eosin staining; both CCM+EGF (top left and right) and M154CF (low left and right) show the Infiltrative BCC pattern: it is represented by many "stripes" of cells that tend to elongate and to spread throughout the tissue.

Both culture media display very well the behavior of this type of tumor: unlike patient 1, the BCC areas in patient 2 are not regular and isolated, but formed by a big web of tumor cells that try to disperse everywhere; sometimes this web is constituted only by lines composed by single cells, as shown in [Fig. 18] top and low right. Both media show very well the architecture and arrangement of the stroma around the cancer, with [Fig. 19] that gives the global image of the tissue right after its excision from the patient.

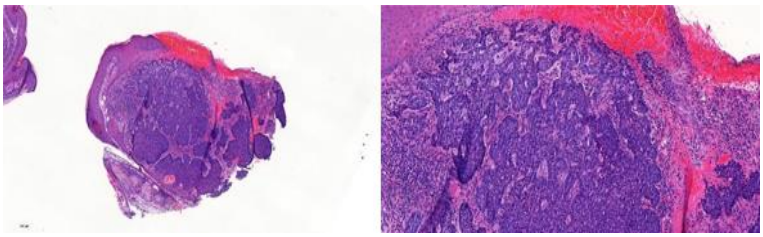

Fig. 19: Patient 2, Hematoxylin-Eosin staining; the Infiltrative-like pattern is confirmed in the H&E test done right after the tissue exportation from the patient (right).

6.2.2 Proliferation Immunofluorescence staining

Regarding proliferation, CCM+EGF shows a central zone where there is a great proliferating activity, while around it is visibly decreased; M154CF instead seems to present a big area with nearly equally distribution of the MKI67

signal, both in the middle and close to the edges, but with a few spotted proliferating cells. This can be fully appreciated in [Fig. 20].

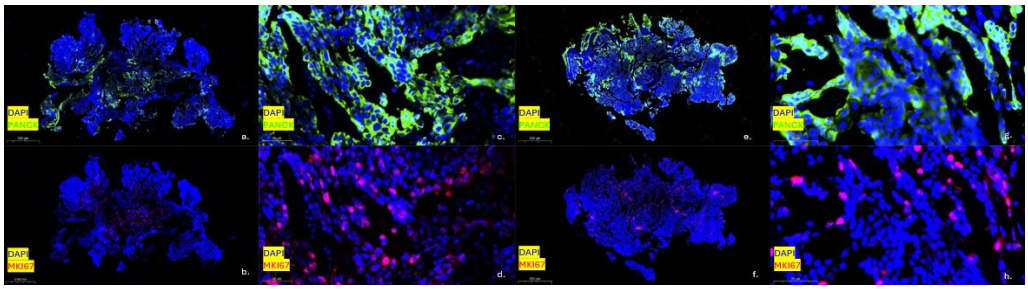

Fig. 20: Patient 2, Proliferation Immunofluorescence staining; in both media the proliferation activity seems quite active but with few differences: CCM+EGF (a., b., c., d.) has a central proliferating core while the perifery seems to have lower biomarker presence, M154CF instead (e., f., g., h.) has more spread signal all around the tissue.

CCM+EGF confirms to be the culture medium with most proliferation for what concerns patient 2. As [Fig. 21 left] indicates, there is a larger number of proliferating cells compared to the whole cancerous cells in the selected areas within the tissue cultured in CCM+EGF, while for M154CF the percentage is half because, as explained before, there are only few spotted-like proliferating cells inside the sample. Different is the situation for the intensity of the biomarker signal: in both culture media it is comparable, in fact there is no significant difference between CCM+EGF and M154CF, as [Fig. 21 right] illustrates.

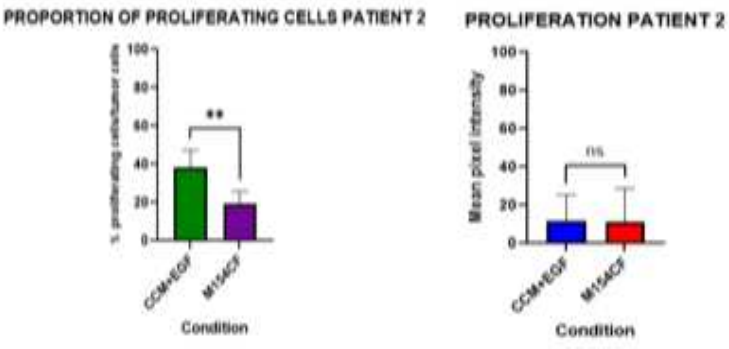

Fig. 21: Patient 2, Proportion of proliferating cells (left) and Mean pixel intensity (right); CCM+EGF has nearly doubled the M154CF looking at the amount of tumor cells with respect to the total cells in the cancerous area; the signal intensity, instead seems to be similar in both media, with no significant difference.

6.2.3 Apoptosis Immunofluorescence staining

Unfortunately, due to practical problems, it was not possible to have acceptable data for the Apoptosis in CCM+EGF, so any comparison cannot be made between the two media.

6.2.4 SPON2-GLI1 FISH staining

Even for patient 2, the first FISH presents a great signal for both the biomarkers; in fact, *GLI1* and *SPON2* are distributed in the whole cancerous tissue, but this time there is no particular concentration in specific areas, like in patient 1, on the contrary, it seems that there is not such a prevalence in any part of the sample; this can be explained by the fact that the tumor is spread all over the tissue without particular zones in which it regroups with other cancerous cells like in patient 1. This can be appreciated in [Fig. 22].

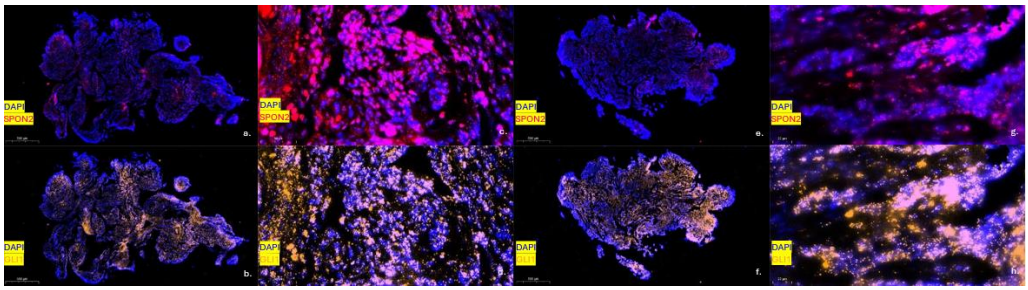

Fig. 22: Patient 2, SPON2-GLI1 FISH staining; both SPON2 (a., c., e., g.,) and GLI1 (b., d., f., h.) are active and well distributed throughout the tissue, giving promising hopes for this test.

Although both signals are sufficiently expressed in both media, *GLI1* has more intensity than *SPON2*. Also, *GLI1* has a great advantage in CCM+EGF, with an intensity signal that almost triples the one expressed in M154CF. On the other side, as [Fig. 23] shows, *SPON2* has less intensity but there is an interesting lead in CCM+EGF with respect to M154CF; it is not proven as a determining signal for BCC detection, but it still might be interesting for future studies.

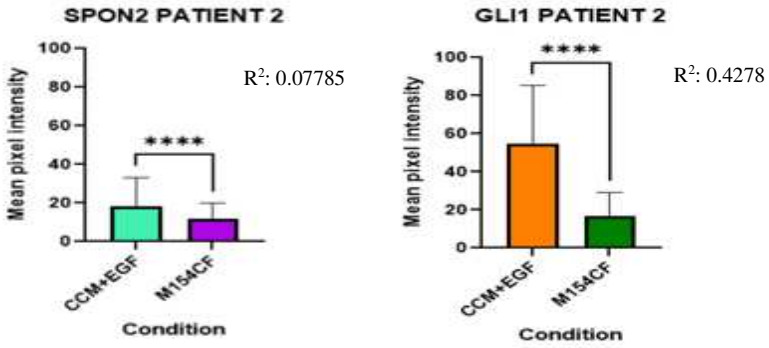

Fig. 23: Patient 2, SPON2 and GLI1 Mean pixel intensities; SPON2 (left) has a significantly greater score in CCM+EGF, as in patient1, while GLI1, although it has very high values, it is nearly equally expressed in both culture media (right).

Analyzing the plotting of *SPON2* and *GLI1* in [Fig. 24], both media have a strongly positive correlation, especially CCM+EGF that reaches 1.248 as *m* coefficient value in the equation of the straight line. Probably this result is due

to *GLI1* that has high scores. However, M154CF is not to be undermined because it also has a remarkable positive correlation, with a *m* value that reaches 1.017 in the equation of the straight line. These results seem to be very promising for future studies with a drug targeting *GLI1*.

y = 1.248 x + 31.87
R^2: 0.3690
p value < 0.0001

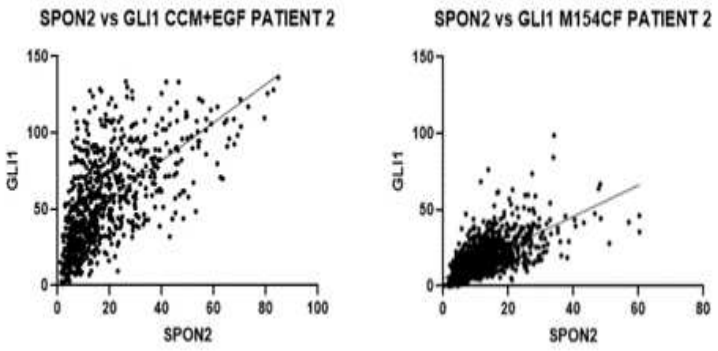

y = 1.017 x + 4.965
R^2: 0.4537
p value < 0.0001

Fig. 24: Patient 2, SPON2-GLI1 correlations; in CCM+EGF (left) the juxtaposed scores are equally distributed, in fact there is a slightly positive correlation between the two; for M154CF, instead, the values are grouped and show a great positive trend (right).

6.2.5 MPPED1-KRT6A FISH staining

Regarding the transition FISH, M154CF seems to have an exceptionally low value compared to CCM+EGF: this might be due to technical problems during the staining of M154CF, but, anyways, the percentages of both *MPPED1* and *KRT6A* are comparable. As for CCM+EGF, [Fig. 25] enlightens well the major expression of *KRT6A* with respect to *MPPED1*, an expected result after all being said about patient 2 peculiarities. Although, there is a relevant *MPPED1* signal that could be related to the transition from Nodular to Infiltrative BCC.

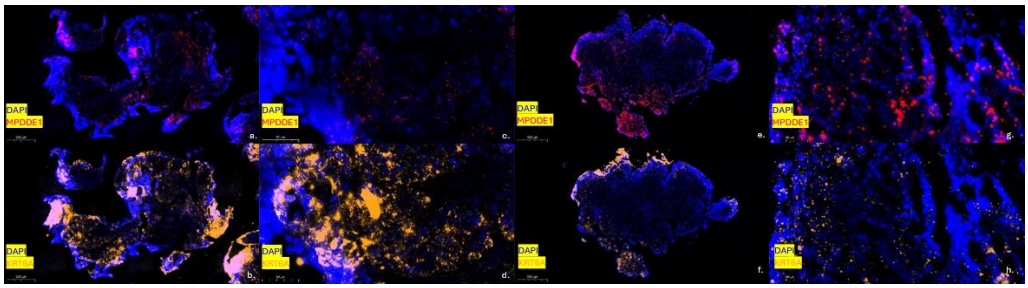

Fig. 25: Patient 2, MPPED1-KRT6A FISH staining; both MPPED1 and KRT6A seem to be majorly expressed in CCM+EGF (a., b., c., d.), with a higher presence of KRT6A (b., d.), due to the Infiltrative-BCC characteristics of the patient; M154CF instead seems to have good presence of both biomarkers on the edges of the tissue (e., f., g., h.) but no signal in the center.

As expected, in [Fig. 26] there is a significant difference between *KRT6A* and *MPPED1* value, with nearly 4 times lead of the first biomarker; in any case, *MPPED1* intensity score is still consistent and can be associated with BCC transition; for M154CF instead, both biomarkers intensities are low and comparable, so it is not sure if there can be a correlation within the two, maybe because of the type of culture medium or the lack of data. These results can be confirmed below, where there is a neat correlation between *MPPED1* and *KRT6A* in CCM+EGF, with the straight line that strengthens the probable degeneration from Nodular to Infiltrative BCC. Although the scores are not high, there is still a slightly positive correlation between the two biomarkers in M154CF, that does not exclude yet the probability of a Nodular-Infiltrative like transition.

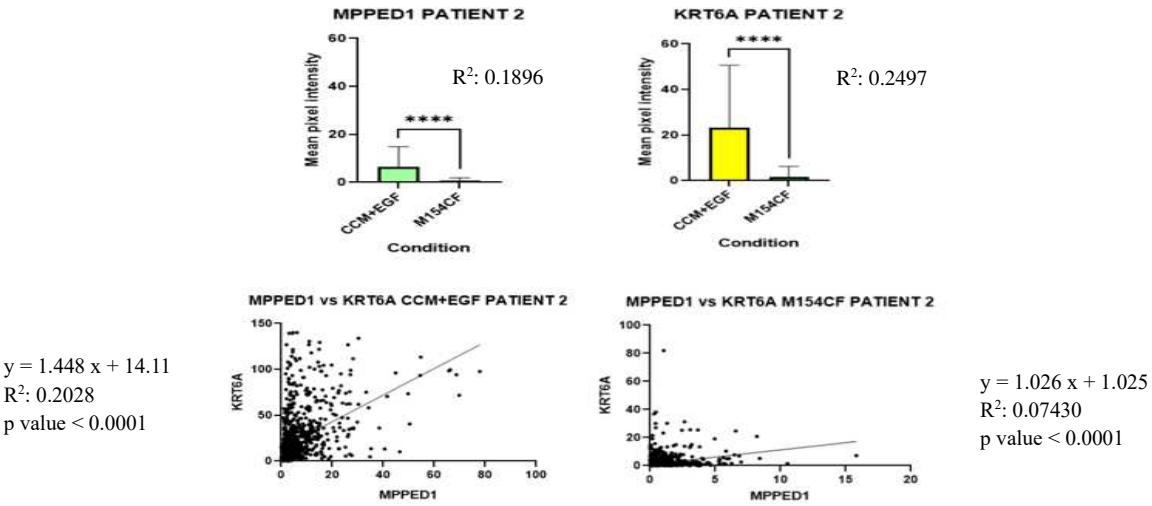

Fig. 26: Patient 2, MPPED1 and KRT6A Mean pixel intensities (top left and right) and biomarker's correlation (low left and right); being an Infiltrative BCC patient, the KRT6A score is higher compared to MPPED1; nevertheless, both biomarkers seem to have a better expression in CCM+EGF with respect to M154CF, maybe due to technical problems. In fact, the correlation between the two markers in CCM+EGF shows a great positive correlation (low left), while for M154CF the correlation is slightly positive (low right).

6.3 Patient 3

6.3.1 Hematoxylin-Eosin staining

The third patient is similar to patient 1 but it also has an interesting feature: it is a sample with a presence of hair follicles, an element that further can disturb the determination of *SPON2-GLI1* FISH staining; with this patient, alongside patient 1 and 2, it is possible to have the widest scenarios possible to grasp BCC and how it is influenced by the surrounding. In [Fig. 27] hair follicles are illustrated with the Hematoxylin-Eosin staining: they show themselves as empty roundish holes that origin within the skin and with time manage to come outside of it.

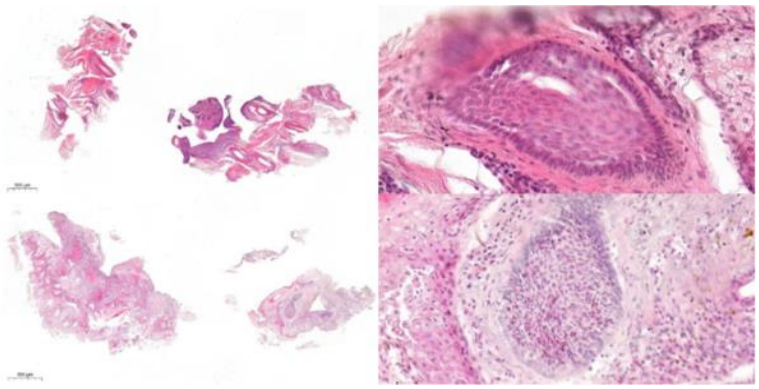

Fig. 27: Patient 3, Hematoxylin & Eosin staining; this patient displays Nodular-BCC features, with the round spotted tumor areas (top and low right); the difference with patient 1 is that here there are many hair follicles around and inside the tumor areas.

Even if not in copious amounts as in patient 1, it seems that patient 3 is also affected by Nodular-BCC. In fact, among the hair follicles, some circular cancerous spots are visible, which can be associated with the typical Nodular-type pattern. In [Fig. 28] it is confirmed the identity of Nodular-BCC through the H&E of the same tissue right after its exportation from the patient.

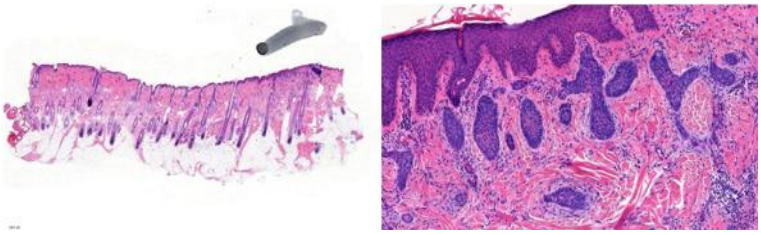

Fig. 28: Patient 3, Hematoxylin & Eosin staining; despite the high presence of hair follicles, the H&E test performed right after the tissue exportation shows the Nodular-BCC pattern.

6.3.2 Proliferation Immunofluorescence staining

Proliferation data are crucial for patient 3 because the situation of the two culture media is completely different: in CCM+EGF, as shown in [Fig. 29 a., b., c., d.], there is a consistent proliferating activity, mostly around the hair follicles bulbs, which at this point of their life cycle, expand very quickly. However, even the tumor areas are well enlightened, thanks to Pan cytokeratin staining, and

even there MKI67 signal is quite high. For M154CF, instead, the signal is incredibly low, probably given by a less presence of hair follicles, but also in the cancerous areas the signal is nearly absent, as [Fig. 29 e., f., g., h.] illustrates.

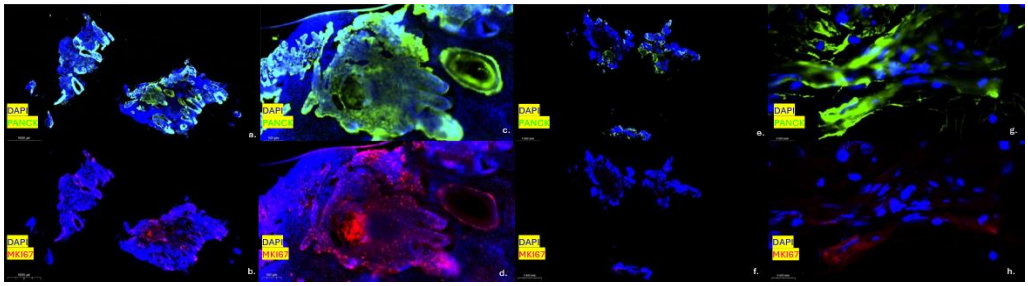

Fig. 29: Patient 3, Proliferation Immunofluorescence staining; tumor areas are concentrated mostly around the hair follicles in CCM+EGF (a., b., c., d.), with a great proliferating activity; M154CF instead (e., f., g., h.) does not have a great signal for both Pan cytokeratin (e., f.) and MKI67 (g., h.).

For proliferation in patient 3, only intensity data are available, but they already confirm what the images above show: proliferation signal in CCM+EGF has a double intensity compared to M154CF and, although the number of proliferating tumor cells is not at hand, it is easy to acknowledge that even that value would be much higher with respect to M154CF where, as seen, it presents only a few red zones. From these assumptions it can be said that CCM+EGF has a higher proliferation rate, as shown in [Fig. 30].

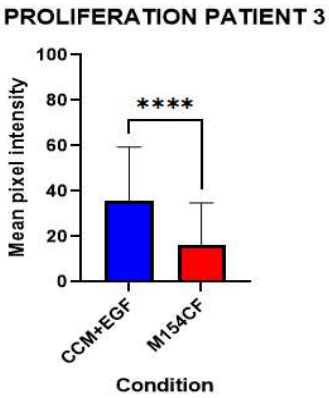

Fig. 30: Patient 3, Proliferation Mean pixel intensity; CCM+EGF has over a significant double score compared to M154CF.

6.3.3 Apoptosis Immunofluorescence staining

Unfortunately, neither for patient 3 apoptosis data are not available because of technical difficulties in the laboratory, so even here the comparison between the two media can be made.

6.3.4 SPON2-GLI1 FISH staining

For what concerns FISH, there is an important aspect to mention: unlike the other patients, *GLI1* is particularly influenced by patient 3 because this sequence can be normally localized in the growing hair follicle area. As seen in [Fig. 31 a., b., c., d.], CCM+EGF, which has more hair follicles within the tissue, has *GLI1* signal inside the tumor areas but especially in the follicle zones; M154CF, having less hair follicles, has a more spread signal, with larger concentrations in the cancerous regions, as for the *SPON2* one ([Fig. 31 e., f., g., h.]).

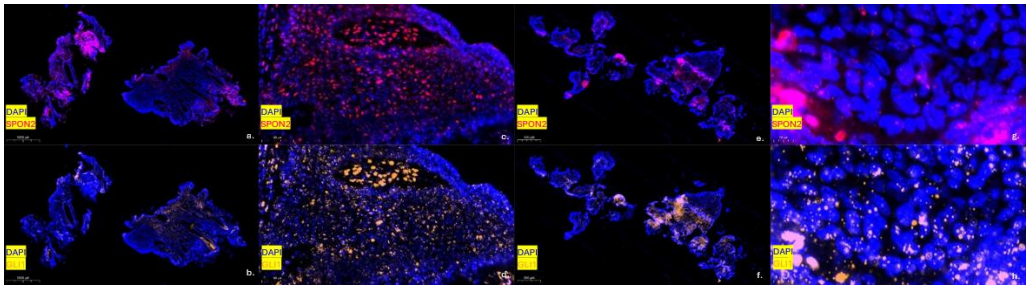

Fig. 31: Patient 3, SPON2-GLI1 FISH staining; also for patient 3, both SPON2 (a., c., e., g.) and GLI1 (b., d., f., h.) have a high signal, especially GLI1, which is normally expressed at hair follicle level.

As [Fig. 32] confirms, *GLI1* signal is more intense in CCM+EGF, which can be explained by the large translation of the mRNA sequence, maybe influenced by the hair follicle growth. For what concerns *SPON2*, the signal is higher in CCM+EGF even if the difference between the two is not so evident. When *SPON2* and *GLI1* are plotted, like below, there is a slightly positive

correlation in both CCM+EGF and M154CF. This could be an interesting result because it is the first time in this study where both media display so low values of the straight-line *m* coefficient, without even reaching 1. Nevertheless, both correlations are positive, meaning that this FISH staining works well.

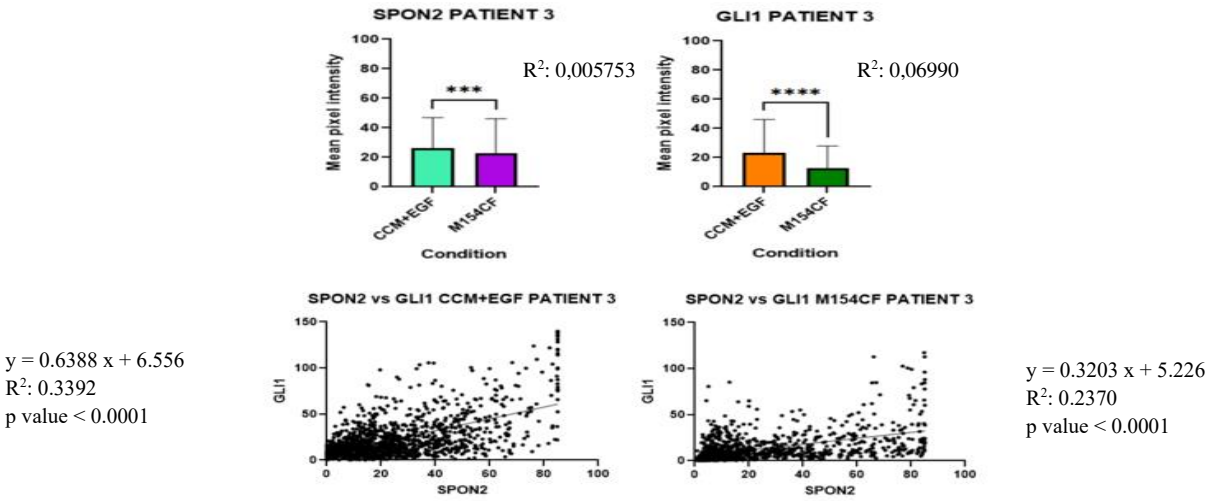

Fig. 32: Patient 3, SPON2 and GLI1 Mean pixel intensities and biomarker's correlations; SPON2 (top left) has similar values in both culture media, while GLI1 has a significantly greater value in CCM+EGF (top right); the biomarker's correlation in CCM+EGF show.

6.3.5 MPPED1-KRT6A staining

Unfortunately, it could not be possible to have sufficient data for the MPPED1-KRT6A FISH staining, so it cannot be possible to draw conclusions about the transition from Nodular to Infiltrative BCC in patient 3.

7 Discussion

All the stains give an idea of the situation for each culture medium for BCC study: regrouping all the data that have been collected, a summary table was done to sum up all the tests performed in this study, indicating which culture medium had the highest score for each biomarker. It seems that CCM+EGF has the most promising future for the future of BCC study, as [Fig. 33] illustrates.

Marker ➞ Patient ⬇	MKI67	Cleaved-Caspase 3	*SPON2*	*GLI1*	*MPPED1*	*KRT6A*
1	M154CF	CCM+EGF	CCM+EGF	CCM+EGF	M154CF	CCM+EGF
2	CCM+EGF	X	CCM+EGF	equal	CCM+EGF	CCM+EGF
3	CCM+EGF	X	equal	CCM+EGF	X	X

Fig. 33: Summary table; all the tests' results are grouped here to see which culture medium performed better in each staining; apart from Proliferation Immunofluorescence and MPPED1 FISH test in patient 1, CCM+EGF had greater scores in all the other tests.

For patient 1 the proliferation level was the highest of all in both culture media, with many cancerous spots that were very active in the proliferation activity, especially in M154CF where the proportion of proliferating cells was over 60 %.

For Apoptosis the values are lower, and even if CCM+EGF has a higher value with respect to M154CF, both results seem to be promising if they are associated with the proliferation ones, because both pairs of value seem to balance each other. To verify which culture medium represents better the physiological environment, it must be compared with the proliferation and apoptotic activity after the tumor exportation, which is not possible.

For the *SPON2-GLI1* staining, both biomarkers are better expressed in CCM+EGF: the higher expression of *GLI1* in this medium is an interesting

outcome because it means that BCC maintains better the Hedgehog pathway activation when cultured in CCM+EGF, compared to M154CF. In both cases, the correlation of the two signals was positive, therefore the test was a success, especially for *SPON2*, which had a consistent score in CCM+EGF, most of all within the tumor areas. Although it is known that it is still not confirmed as a marker associated with BCC insurgence, this study could be object of further investigation for its relationship with the tumor.

The transition FISH staining reveals a possible degeneration from Nodular to Infiltrative BCC in both culture media. Clearly in patient 1 *MPPED1* was the most represented being a Nodular-BCC patient, but in the areas with both signals there is a prevalence of *KRT6A*; even if the score is not extremely high, this may suggest a transition from the Nodular tumor to the Infiltrative one, as confirmed by the slightly positive trend of both media in the correlation graph ([Fig. 34]).

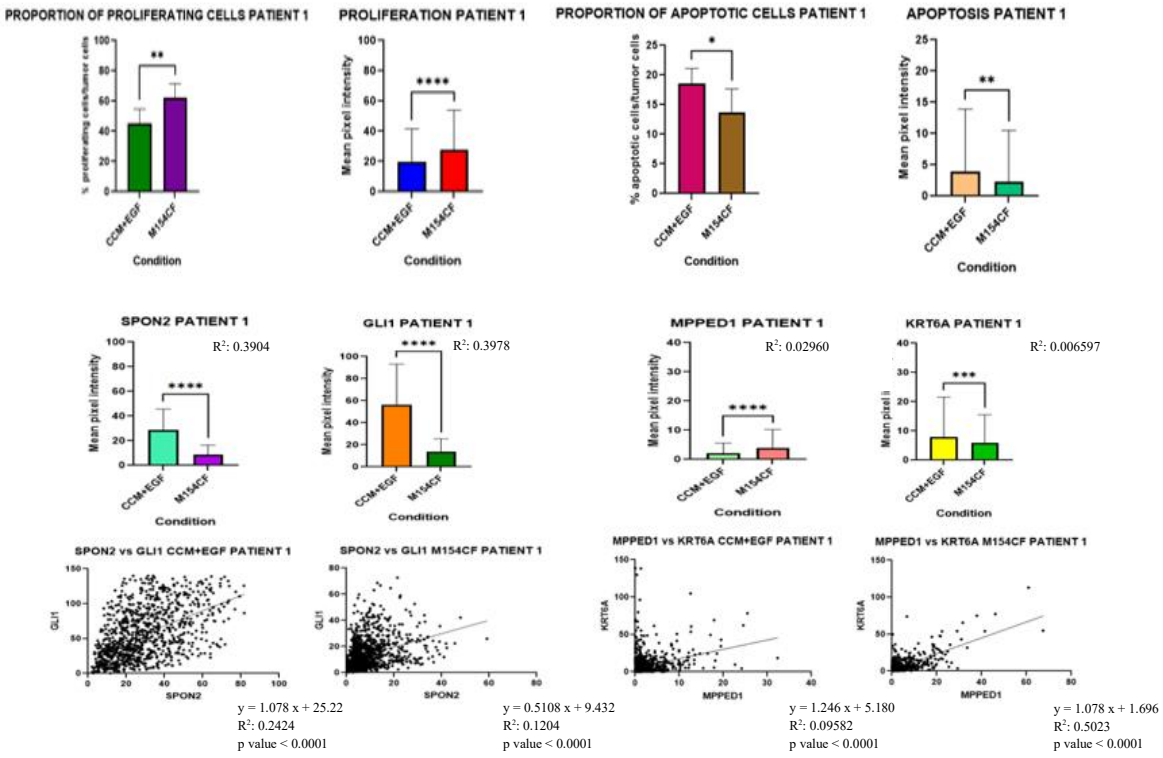

Fig. 34: Patient 1 tests' results summarized; CCM+EGF has better scores, except for Proliferation assay and MPPED1 Mean pixel intensity; all SPON2-GLI1 and MPPED1-KRT6A correlations show a positive trend.

Patient 2 as well had a remarkably proliferation level but, unlike patient 1, CCM+EGF had a higher score compared to M154CF. This is interesting because, although both tissues had an Infiltrative-like core, CCM+EGF favored the expansion of the tumor through a high proliferation rate, while M154CF did not because it had low proliferating signals distributed throughout the whole sample even if the intensity of the apoptotic activity was the same for both culture media.

Despite the absence of Apoptosis data, the FISH stains gave important results since *GLI1* has a great intensity score in CCM+EGF; even here *SPON2* plays a satisfying role because in CCM+EGF is majorly expressed, which might be interesting because it is a gene sequence greatly transcribed in both types of BCC. These satisfying results are confirmed by the positive correlation between the two biomarkers, especially for CCM+EGF which has a steeper straight line.

For what concerns the transition FISH, CCM+EGF has a neat pattern because *KRT6A* signal is over 20 Mean pixel intensity and *MPPED1* above 5: these results highly suggest that there is a degeneration from a once Nodular BCC to an Infiltrative one in the present, thanks also to the plotting of the two signals in the XY graph, which emphasize the highly positive correlation. For M154CF we have also a positive correlation, even if not enlightening as CCM+EGF, also because both biomarkers had a little signal all over the whole tissue area ([Fig. 35]).

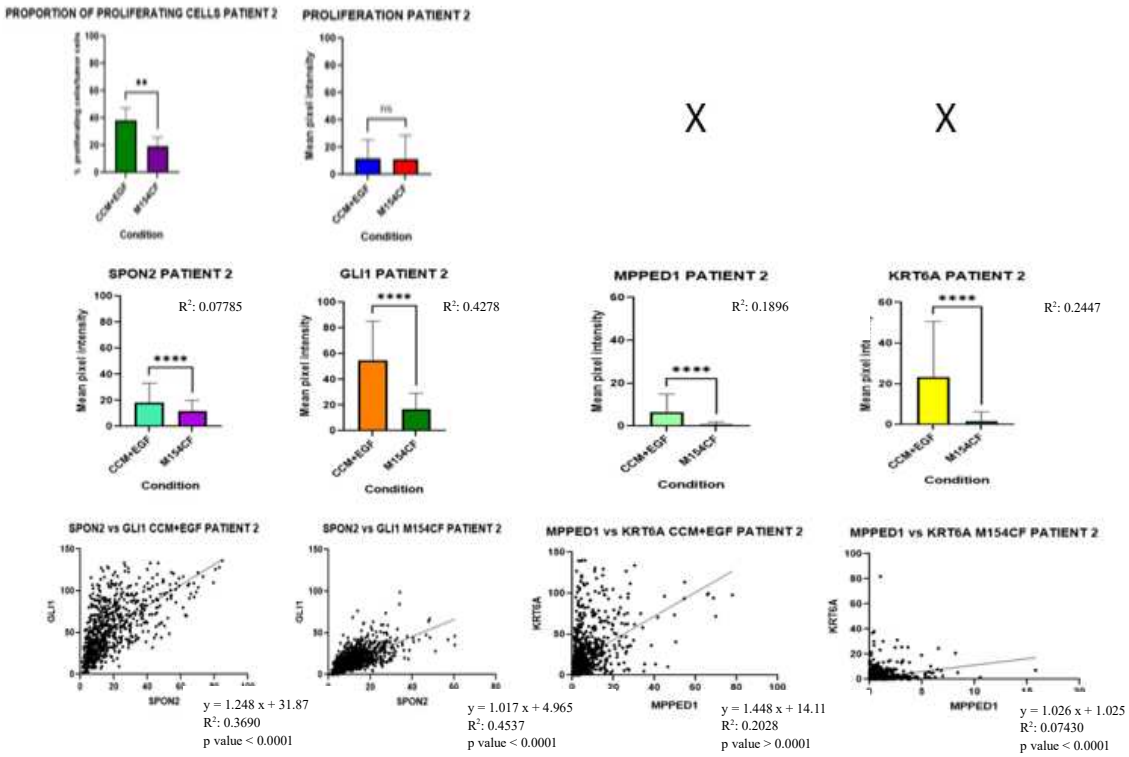

Fig. 35: Patient 2 tests' results summarized; all results suggest an advantage of CCM+EGF, apart for the Proliferation and GLI1 Mean pixel intensities, where the signals do not show any significant difference. The correlation graphs show an overall positive correlation.

Patient 3 was curious to analyze by the presence of hair follicles in the tissue, determining factors that could interfere with BCC determination, due to their high proliferation and *GLI1* expression, biomarkers that are shared between both the expanding hair follicle and BCC insurgence and could be confused during the calculations. Nevertheless, the proliferation rate was quite high,

especially in CCM+EGF; the intensity of the proliferating signal here was around 40 mean pixel intensity, compared to M154CF.

Although unfortunately it was not possible to collect valid data for both Apoptosis and transition FISH for patient 3, the *SPON2*-*GLI1* FISH staining was very interesting because both the biomarkers were present in the tumor areas and in the origin point of the follicle's growth. *GLI1* had a consistent presence in the hair follicle where, as expected, the mRNA sequence is physiologically transcribed, but also in the cancerous areas around, where it reached nearly a 20 % score for CCM+EGF. *SPON2* also was relevant, in fact in both culture media it went over 20 Mean pixel intensity points and was also present in both hair follicles. Most importantly it was expressed in the spotted BCC areas, so eventually all three patients displayed a good correlation between the presence of BCC and the expression of *SPON2* sequence. Even for patient 3, the correlation between *GLI1* and *SPON2* is positive, with CCM+EGF that has a more convincing positive trend ([Fig. 36]).

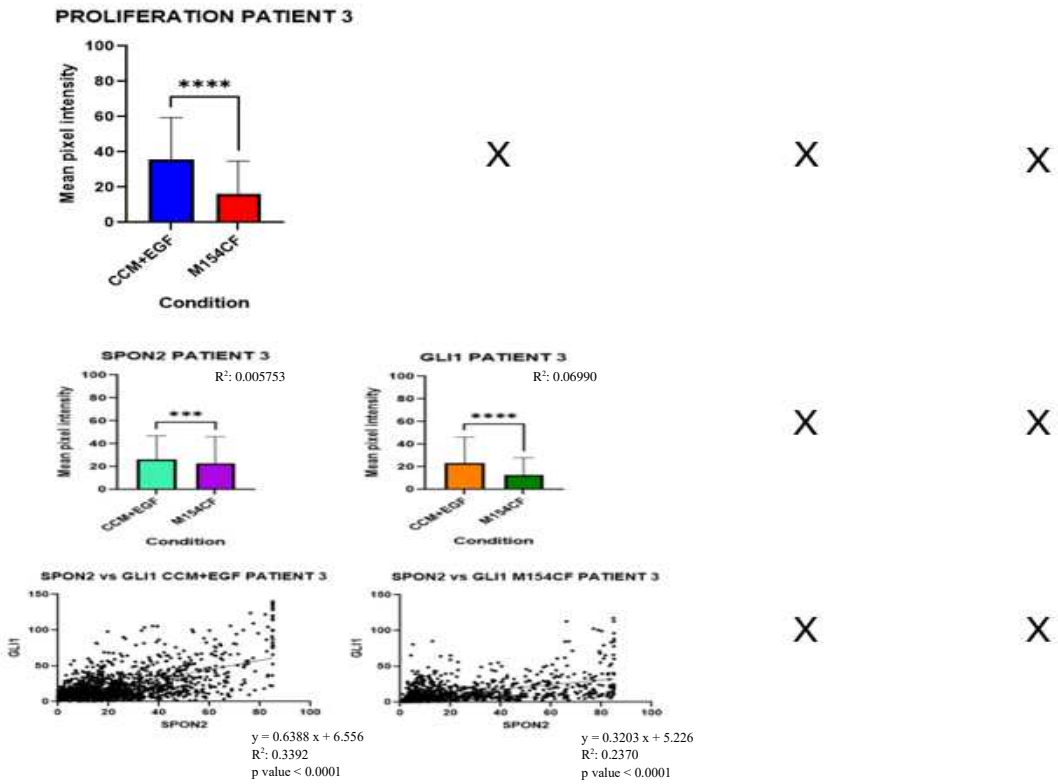

Fig. 36: Patient 3 tests' results summarized; only Proliferation Mean pixel intensity and SPON2-GLI FISH calculations are available. CCM+EGF displays higher values, except for the SPON2 Mean pixel intensity where the results are comparable. The biomarker's correlations have a positive trend, especially in CCM+EGF where it is better enlightened.

Finally, three different graphs were plotted, ([Fig. 37]) where each biomarker of each patient was assembled and characterized only by the culture medium.

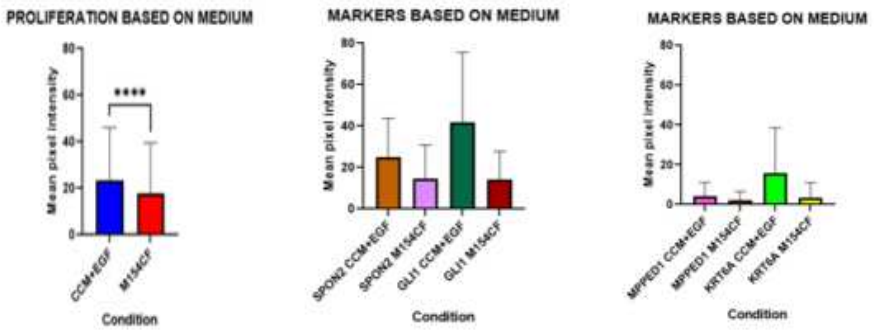

Fig. 37: Proliferation, SPON2-GLI1 and MPPED1-KRT6A FISH stains compared based on the medium; all the data collected from all the patients show a higher score for CCM+EGF.

These graphs once and for all confirm that each marker is best expressed in CCM+EGF, sometimes with a little difference, like in the proliferation graph, other times with a larger distance, as in the transition FISH, where the *KRT6A* is way ahead in CCM+EGF compared to M154CF.

8 Conclusions

CCM+EGF has best results in almost every field of this study, except for Proliferation and *MPPED1* determinations in patient 1 where the values are lower. It is reminded that having higher scores does not mean that the culture medium is better, the best culture medium is the one that better represents the physiological environment. Although H&E images were available to confront with the one obtained during this study, the images of Proliferation, Apoptosis and both FISHes were not available to compare with the ones stained for this work. Consequently, it is possible only to say that BCC+EGF, having higher values in most of the stains, can be used in the future for further studies with a Hedgehog inhibitor drug (ex. Vismodegib), because the contrast between high signal and lower signal due to the drug, could be better appreciated.

As for this study, it can be assumed that the two culture media are different from each other. It is not possible to determine what culture medium is better, however, both media influence diversely the tumor explants and this gives courage for future studies on this issue, with a drug's help that could cast light upon this topic.

Bibliography

1. Gallo, R. L. Human Skin Is the Largest Epithelial Surface for Interaction with Microbes. *J. Invest. Dermatol.* **137**, 1213–1214 (2017).
2. Solano, F. Metabolism and Functions of Amino Acids in the Skin. in *Amino Acids in Nutrition and Health* (ed. Wu, G.) vol. 1265 187–199 (Springer International Publishing, Cham, 2020).
3. Grice, E. A. & Segre, J. A. The skin microbiome. *Nat. Rev. Microbiol.* **9**, 244–253 (2011).
4. Wong, R., Geyer, S., Weninger, W., Guimberteau, J. & Wong, J. K. The dynamic anatomy and patterning of skin. *Exp. Dermatol.* **25**, 92–98 (2016).
5. Nguyen, A. V. & Soulika, A. M. The Dynamics of the Skin's Immune System. *Int. J. Mol. Sci.* **20**, 1811 (2019).
6. Kolimi, P., Narala, S., Nyavanandi, D., Youssef, A. A. A. & Dudhipala, N. Innovative Treatment Strategies to Accelerate Wound Healing: Trajectory and Recent Advancements. *Cells* **11**, 2439 (2022).
7. Nourian Dehkordi, A., Mirahmadi Babaheydari, F., Chehelgerdi, M. & Raeisi Dehkordi, S. Skin tissue engineering: wound healing based on stem-cell-based therapeutic strategies. *Stem Cell Res. Ther.* **10**, 111 (2019).
8. Anastasi, G. *et al. TRATTATO DI ANATOMIA UMANA*. vol. 1 (Edi.Ermes s.r.l., Milano, 2006).
9. Rinnerthaler, M., Bischof, J., Streubel, M., Trost, A. & Richter, K. Oxidative Stress in Aging Human Skin. *Biomolecules* **5**, 545–589 (2015).

10. epidermis anatomy. layers and Cell structure vector de Stock. *Adobe Stock* https://stock.adobe.com/es/images/epidermis-anatomy-layers-and-cell-structure/445861813.
11. Brand, A., Hovav, A. & Clausen, B. E. Langerhans cells in the skin and oral mucosa: Brothers in arms? *Eur. J. Immunol.* **53**, 2149499 (2023).
12. Bataille, A., Le Gall, C., Misery, L. & Talagas, M. Merkel Cells Are Multimodal Sensory Cells: A Review of Study Methods. *Cells* **11**, 3827 (2022).
13. How to choice the best hyaluronic acid for Hyaluron Pen needle free injection. *Wassup Apgujeong Korean Skin Care Reviews* https://www.korean-surgery.com/best-dermal-fillers-for-hyaluron-pen-needle-free-injection/ (2019).
14. Zhang, B. & Chen, T. Local and systemic mechanisms that control the hair follicle stem cell niche. *Nat. Rev. Mol. Cell Biol.* **25**, 87–100 (2024).
15. Schneider, M. R., Schmidt-Ullrich, R. & Paus, R. The Hair Follicle as a Dynamic Miniorgan. *Curr. Biol.* **19**, R132–R142 (2009).
16. Struktur und Zyklen der Haarwuchs auf dem menschlichen Kopf unter... *iStock* https://www.istockphoto.com/de/vektor/struktur-und-zyklen-der-haarwuchs-auf-dem-menschlichen-kopf-unter-einem-mikroskop-gm1130772706-299177939 (2019).
17. Madaan, A., Verma, R., Singh, A. T. & Jaggi, M. Review of Hair Follicle Dermal Papilla cells as *in vitro* screening model for hair growth. *Int. J. Cosmet. Sci.* **40**, 429–450 (2018).

18. Martel, J. L., Miao, J. H., Badri, T. & Fakoya, A. O. Anatomy, Hair Follicle. in *StatPearls* (StatPearls Publishing, Treasure Island (FL), 2024).
19. Liu, Y. *et al.* Hedgehog signaling reprograms hair follicle niche fibroblasts to a hyper-activated state. *Dev. Cell* **57**, 1758-1775.e7 (2022).
20. Anatomische Ausbildung Plakat. Wachstumsphase der Haare Schritt für... *iStock* https://www.istockphoto.com/de/vektor/anatomische-ausbildung-plakat-wachstumsphase-der-haare-schritt-f%C3%BCr-schritt-phasen-gm926246448-254157139 (2018).
21. Avery, J. T., Zhang, R. & Boohaker, R. J. GLI1: A Therapeutic Target for Cancer. *Front. Oncol.* **11**, 673154 (2021).
22. Zhang, X. *et al.* The SHH-GLI1 pathway is required in skin expansion and angiogenesis. *Exp. Dermatol.* **32**, 1085–1095 (2023).
23. Cameron, M. C. *et al.* Basal cell carcinoma. *J. Am. Acad. Dermatol.* **80**, 303–317 (2019).
24. Hernandez, L. E. *et al.* Basal cell carcinoma: An updated review of pathogenesis and treatment options. *Dermatol. Ther.* **35**, (2022).
25. Basset-Seguin, N. & Herms, F. Update in the Management of Basal Cell Carcinoma. *Acta Derm. Venereol.* **100**, adv00140 (2020).
26. Carballo, G. B., Honorato, J. R., De Lopes, G. P. F. & Spohr, T. C. L. D. S. E. A highlight on Sonic hedgehog pathway. *Cell Commun. Signal.* **16**, 11 (2018).
27. Frampton, J. E. & Basset-Séguin, N. Vismodegib: A Review in Advanced Basal Cell Carcinoma. *Drugs* **78**, 1145–1156 (2018).

28. Zito, P. M., Nassereddin, A. & Scharf, R. Vismodegib. in *StatPearls* (StatPearls Publishing, Treasure Island (FL), 2024).
29. Alkeraye. Vismodegib for Basal Cell Carcinoma and Beyond: What Dermatologists Need to Know. *Cutis* **110**, (2022).
30. Sanmartín, O. *et al.* Sonidegib en el tratamiento del carcinoma basocelular localmente avanzado. *Actas Dermo-Sifiliográficas* **112**, 295–301 (2021).
31. Dummer, R. *et al.* Long-term efficacy and safety of sonidegib in patients with advanced basal cell carcinoma: 42-month analysis of the phase II randomized, double-blind BOLT study. *Br. J. Dermatol.* **182**, 1369–1378 (2020).
32. Chan, J. K. C. The Wonderful Colors of the Hematoxylin–Eosin Stain in Diagnostic Surgical Pathology. *Int. J. Surg. Pathol.* **22**, 12–32 (2014).
33. *Oral Biology: Molecular Techniques and Applications*. vol. 2588 (Springer US, New York, NY, 2023).
34. Im, K., Mareninov, S., Diaz, M. F. P. & Yong, W. H. An Introduction to Performing Immunofluorescence Staining. in *Biobanking* (ed. Yong, W. H.) vol. 1897 299–311 (Springer New York, New York, NY, 2019).
35. Bahry, E. *et al.* RS-FISH: precise, interactive, fast, and scalable FISH spot detection. *Nat. Methods* **19**, 1563–1567 (2022).
36. SPON2. *Early Detection Research Network* https://edrn.nci.nih.gov/data-and-resources/biomarkers/spon2/.
37. *RNA Detection and Visualization: Methods and Protocols*. vol. 714 (Humana Press, Totowa, NJ, 2011).

38. Kułak, K., Wojciechowska, N., Samelak-Czajka, A., Jackowiak, P. & Bagniewska-Zadworna, A. How to explore what is hidden? A review of techniques for vascular tissue expression profile analysis. *Plant Methods* **19**, 129 (2023).
39. Menz, A. *et al.* Pan-keratin Immunostaining in Human Tumors: A Tissue Microarray Study of 15,940 Tumors. *Int. J. Surg. Pathol.* **31**, 927–938 (2023).